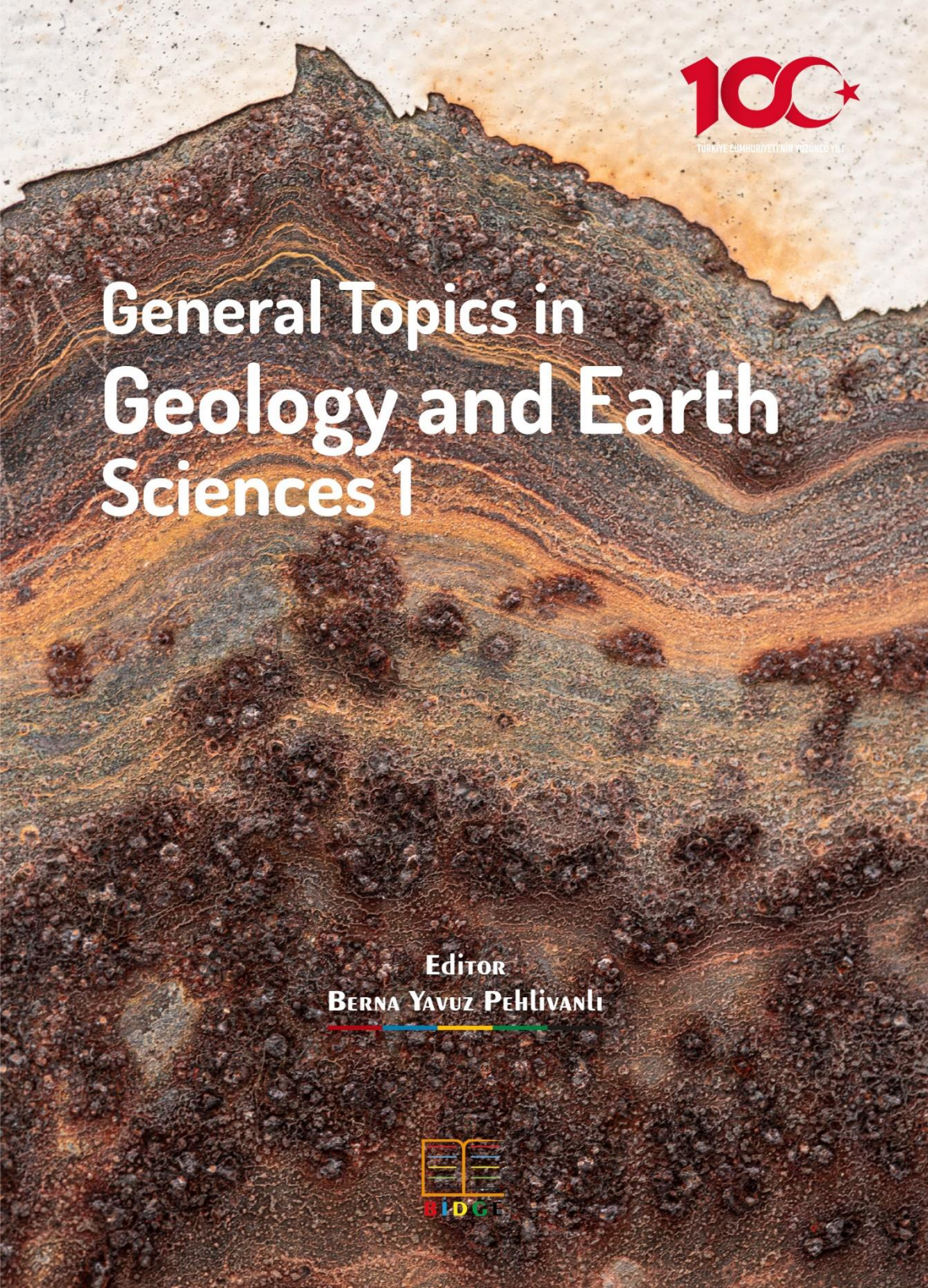
100
TÜRKİYE CUMHURİYETİ'NİN YÜZÜNCÜ YILI
General Topics in
Geology and Earth
Sciences 1
Editor
Berna Yavuz Pehlivanli
BİDGE

BIDGE Publications

General Topics in Geology and Earth Sciences 1

Editor: Doç. Dr. Berna Yavuz Pehlivanlı

ISBN: 978-625-6645-64-6

Page Layout: Gözde YÜCEL

1st Edition:

Publication Date: 25.12.2023

BIDGE Publications,

www.bidgeyayinlari.com.tr - bidgeyayinlari@gmail.com

Krc Bilişim Ticaret ve Organizasyon Ltd. Şti.
Güzeltepe Mahallesi Abidin Daver Sokak Sefer Apartmanı No: 7/9 Çankaya / Ankara

Contents

CHAPTER I

Alkaline Igneous Rocks

Abdullah SAR[1]
Mehmet Ali ERTÜRK[2]
Cihan YALÇIN[3]

Introduction

Alkaline is defined as having a higher alkali concentration than in feldspar alone. It also describes rocks containing significant amounts of foids (nepheline, sodalite, leucite), alkaline pyroxenes, alkaline amphiboles, and melilite. Alkaline rocks generally contain more alkali than the feldspars alone can carry. Excess alkalis occur in feldspathoids, sodic pyroxenes-amphiboles or other alkali-rich

[1] Dr. Arş. Gör., Fırat University, Engineering Faculty, asar@firat.edu.tr ORCID No: 000-0002-9752-7807
[2] Dr. Öğr. Üyesi, Fırat University, Engineering Faculty, erturkmae@gmail.com ORCID No: 0000-0003-1197-9202
[3] Dr., Ministry of Industry and Technolgy, Wordbank PIU. cihan.yalcin@sanayi.gov.tr ORCID No: 0000-0002-0510-2992

phases. In the most limited sense, alkaline rocks are so deficient in SiO_2 as to become critically unsaturated concerning Na_2O, K_2O, and CaO, with Nepheline or Acmite appearing to be the norm.

On the other hand, some rocks may be deficient in Al_2O_3 (and not necessarily SiO_2), so Al_2O_3 may not accommodate the alkalis in normative feldspars. Such rocks are called peralkaline; the silica can be undersaturated or oversaturated (URL-1). Compared to alkalis, these rocks are insufficient in silica and alumina, and their norms contain nepheline and akmite. For example, carbonatites are certainly poor in silica but rarely rich in alkali. True (nepheline normative) alkaline basalts transform into hypersthene normative transitional basalts without any significant change in mineralogy. Because transitional basalts are often closely associated with alkaline basalts in the field, they are traditionally considered alkaline. It is practical to define alkaline igneous rocks simply by their alkaline (Na_2O+K_2O) and silica contents (Fitton & Upton, 1987).

Alkaline rocks can be grouped as follows:

1) Rocks containing sufficient or excess silica lacking alumina: These rocks with a molecular ratio of $(Na_2O+K_2O)/Al_2O_3 > 1$ are called peralkaline rocks. Typical peralkaline silicic volcanics are represented by pantellerite (Na-rich rhyolite) and comendite (K-rich rhyolite) (URL-1).

2) Rocks in which alumina is sufficient (enough to saturate the feldspar composition) or in excess, but silica is deficient: The rocks then consist of feldspars and feldspathoids, as well as mica hornblende, corundum, etc. Tephrite and phonoliths fall into this group (URL-1).

3) Rocks deficient in both silica and alumina according to feldspar composition: Rocks contain alkali feldspars, as well as silica-unsaturated minerals, feldspathoids, and alkali-rich mafic minerals. Foid-containing trachytes belong to this group (URL-1).

Various aspects of the classification of alkaline rocks need to be clarified and controversial. This reflects uncertainty about genetic relationships and the tectonic setting of many formations. While some researchers attempt classification based on genetic similarities (such as igneous series), others recognize the difficulty of assessing the formation of such diverse rocks in complex continental environments and use chemical, mineralogical, mineralogical, and textural similarities (URL-1).

Alkaline Igneous Rocks

Carbonatites

Carbonatite is a rare rock type that is considered to be of mantle origin, rich in calcite and other carbonate minerals. Igneous rocks containing more than 50% carbonate minerals are defined as carbonatites (Figure 1). These rocks are found in association with intruded masses, dykes, conical covers, and rarely lavas and tephra, in association with alkali-rich red rocks (such as nepheline, syenite). Carbonatite formations are highly prevalent as either intrusive or sub-volcanic rocks. Carbonatites associated with alkaline intrusive complexes are mostly seen as zoned stocks, sills, dykes, breccias and veins. They are seperated into subunits depending on their carbonate (calcite, dolomite and ankerite) and silicate (biotite, pyroxene, amphibole, etc.) mineral contents (Pirajno, 2022; Yastı, 2023). Volcanic derivatives are rare. Because the flow of carbonatite lavas is irregular, they react with the atmosphere very quickly. The oldest known active carbonatite volcano is the Ol Doinyo Lengai volcano in Tanzania. This volcano ejected lava with the lowest temperature in the world (500°C-600°C) (URL-2; Yastı, 2023).

Rarely seen carbonatites are geochemically rich in high amounts of Ba, Sr, P and light-REE. Carbonatites are characteristically located in systems associated with alkali silicate magmatic rocks. Associated silicates are generally alkaline ultramafic rocks. They may mostly contain more evolved types such as pyroxenites, nephelinites (and ijolites), and, to a lesser extent,

phonolite and nepheline syenite (URL-2; Yastı, 2023). There are essentially three main theories regarding the origin of carbonatites:

1. Fractionated carbonated nephelinite or melilite residue melts.

2. Immiscible melt fractions of CO2-saturated silicate melts.

3. Primary mantle melts formed by partial melting of peridotite containing CO_2.

A combination of these three theories is also popular. For example, carbonatite melts formed by deep melting of carbonate eclogite in the upper mantle infiltrate peridotites to produce silica-poor carbonate-containing melts, which then penetrate the crust and evolve or decompose (Yaxley & Brey, 2004; Yastı, 2023). Carbonatites are also thought to be formed in the lithospheric mantle as rapidly emerging partial melts due to hot mantle uplift. If the rate of this mantle carbonate melting decreases due to sudden heat loss, carbonate melt metasomatism occurs in the mantle. Approaching the much hotter centre of the crest causes melting in the metasomatic plane, and the formation of carbonatite melts is observed on the surface. Although the crest model is widely accepted, the age distributions of carbonatites determined worldwide in recent years have been strongly lithospherically controlled, suggesting a direct connection with mantle crests. (Woolley & Bailey, 2012; Yastı, 2023).

The atomic structures of carbonate ranges have yet to be studied compared to the structures of silicate ranges. Still, they play a fundamental role in controlling their chemical and physical behaviour in natural systems. The atomic structures of carbonate melts are essential in controlling physical and chemical behaviour in natural systems but have yet to be investigated compared to silicate melts. Ionic carbonate melts are thought to contain a structural disorder in which there is no obvious relationship between metal cations and carbonate molecules. However, when data on the phase relationships of carbonates, the solubility of metals in carbonate

liquids, and spectroscopy and atomic simulations of carbonate glasses are combined, it emerges that carbonate liquids have structures on a larger scale than their component molecular groups. Factors controlling the crystallization of carbonatite-alkali complexes;

- direct production by very low-grade partial melting and melt differentiation in the mantle,
- liquid immiscibility between a silicate melt and a carbonate melt,
- peculiar, extremely crystalline fractionation (URL-2; Yastı, 2023).

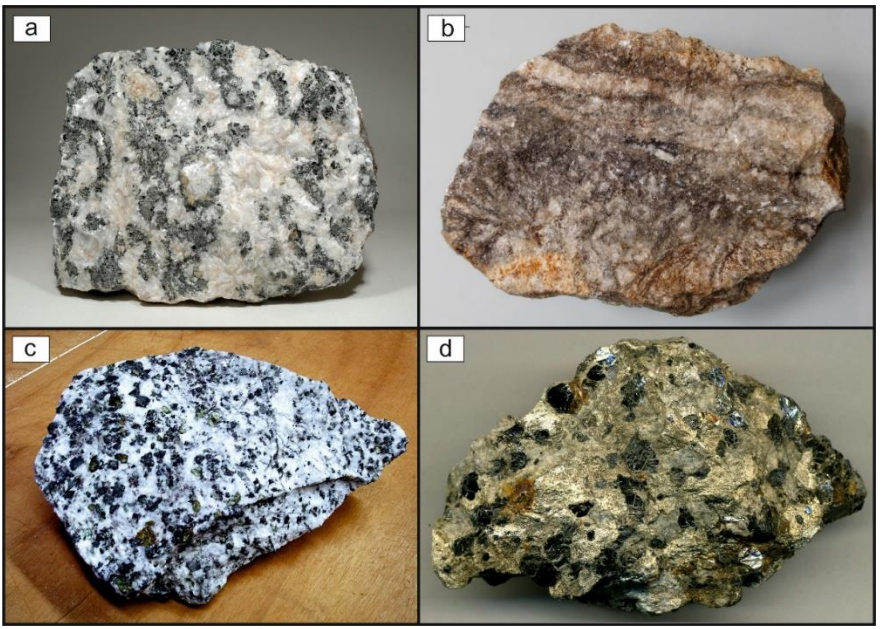

Figure 1. Macroscopic views of carbonatites (URL-2; URL-3)

Although there is data about each process, the main point is that these models are unusual and special processes. Considering the geochemical and mineralogical data, it is thought that carbonatites were formed by magma melting limestone or marble during intrusion.

Silicates intruding into the host rocks cause phenitization in the host rocks. Fenitization is an indicator of alteration and consists of green-coloured, alkali feldspar, egyrin and alkali hornblende dominant rocks. Fenitization occurs during the crystallization of carbonatites containing highly alkaline elements and volatile components.

Carbonatites are classified as calcite sovite (coarser textured) and alvicite (finer textured) types or facies. The two are also distinguished by their trace and minor element composition (Le Bas, 1999; URL-2). Alkaline carbonatites are called lengaites. Samples containing 50-70% carbonate minerals are called in-silico carbonatites (Kresten, 1983). Additionally, carbonatites may be enriched in apatite and magnetite or rare earth elements, fluorine and barium (Guilbert et al., 1986; URL-2).

Natrocarbonatite consists largely of two minerals: nyerereite and gregorite. These minerals are carbonates in which both sodium and potassium are present in significant amounts. Both are anhydrous and react extremely quickly when they come into contact with moisture in the atmosphere. Erupting dark brown or black lava and ash, which begins to turn white within a few hours, then turns grey after a few days and brown after a few weeks (Allington-Jones, 2014; URL-2)

Nephelinites

They are fine-grained extrusive rocks composed of nepheline and clinopyroxene (Figure 2); Nephelinites in which mafic minerals are more abundant than foids are called melanephelinites. Cordier first used the term in 1842 (URL-1).

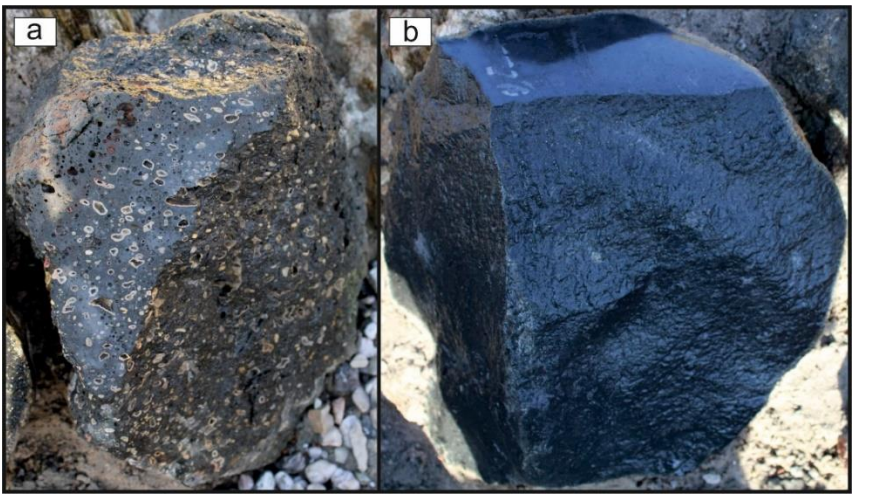

Figure 2. Macroscopic views of nephelinites (URL-4; URL-5)

Nephelinites (along with melilitids and more exotic types such as kamafugites and alnoids) generally occur in continental rift zones, sometimes associated with carbonatites, but are also found on oceanic islands and some subduction environments. Experimental studies have revealed that they are the product of low-grade melting at high CO_2 pressures (Brey and Green, 1975). However, their ultimate origin and relationships with more ordinary alkaline basalts must be fully understood (Zeng et al. 2021).

Lamprophyres

Lamprophyres are a complex group of rocks showing mineralogical similarities to kimberlites and lamproites (Figure 3) (URL-6). Lamprophyres are difficult to classify using existing criteria. They can not be classified according to modal ratios such as the QAPF system or compositional discrimination diagrams such as TAS. It is unlikely that a simple taxonomic system will be found unless appropriate genetic criteria are applied, unless the classification considers the formation of rocks. The term "lamprophyre", from "lampros" and "porphyry" (shiny porphyry), was introduced by von Gumbel in 1874 for a group of dark rocks

forming small depressions containing phenocryst brown mica and hornblende, but not feldspar phenocrysts. Following its definition, the term was expanded to include various hypabyssal rocks containing ferromagnesian phenocrysts. As the number of difficult rocks to classify increased in the late 19^{th} and early 20^{th} centuries, they were added to the lamprophyre group (URL-6). Eventually, the group became a repository for mafic phenocryst-rich rocks that are difficult to characterize. Unfortunately, applying type locality nomenclature has led to "a legion of obscure rock types named after equally obscure European villages". This archaic, often imprecise terminology has been a particular obstacle in lamprophyre petrogenetic studies due to the grouping of rocks of different lineages under a single petrographic heading. This grouping has been interpreted to imply genetic relationships that do not exist (URL-6).

"Lamprophyres are rocks characterized by the presence of euhedral to submorphic phenocrysts composed of mica and amphibole, with lesser amounts of clinopyroxene and melilite, embedded in a matrix that may consist of plagioclase, alkali feldspar, carbonate, feldspathoids, melilite, monticellite, mica, pyroxene perovskite, amphibole, Fe-Ti oxides and glass" (URL-6).

Lamprophyres are divided into four groups;

• Calc-alkaline (shoshonitic) lamprophyres.

• Leucite lamprophyres.

• Alkaline lamprophyres.

• Ultramafic lamprophyres.

Calc-alkaline (shoshonitic) lamprophyres

These are nearly saturated, slightly potassic (Na < K) lamprophyres with moderate SiO_2 content (about 53%) and accompany most post-orogenic granites or slightly potassic (shoshonitic) alkaline rocks. Their mineralogy, chemistry, field relationships, Sr isotopic ratio, and xenolith content have been taken to proposed that they are typically hybrids between granitic debris or

crustal sediments and basic magma. Calc-alkaline lamprophyres are also known as ordinary lamprophyres and consist of minette, vosegit, kersantite and spessartite (URL-6).

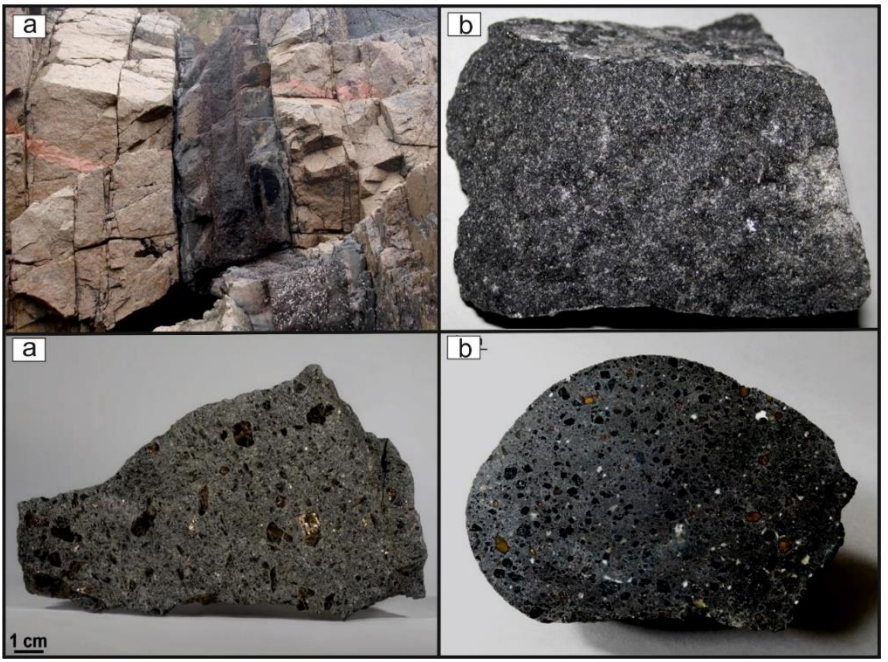

Figure 3. Macroscopic views of lamprophyres (URL-6)

Vosegites: A vogesite, basic amphibole, is a porphyritic alkaline igneous rock dominated by hornblende and potassic feldspar, often with augite and plagioclase present as accessories in the groundmass.

Minettes: Minette is a porphyritic alkaline igneous rock dominated by elemental biotite and potassium.

Leucite lamprophyres

Leucite lamprophyres are often described as "lamprophyric" due to their porphyritic character and large biotite or magnophorite phenocrysts. Some are near saturation, do not differ from minenets, and fall into the broad category of potassic alkaline rocks. However,

their similarities are unclear, and their petrogenesis is quite different from other lamprophyre groups (URL-6).

Cascadite: Cascadite is a sodic melanocratic lamprophyre consisting of biotite, olivine and augite phenocrysts in a matrix consisting mainly of alkali feldspar and containing fragments that may be leucite (URL-6).

Fitzroydite: Fitzroydite is a leucite-phlogopite lamprophyre (URL-6) consisting mainly of phlogopite and leucite.

Orendite: Orendite is leucite lamprophyre composed primarily of leucite, alkali feldspar, and, secondarily, clinopyroxene, mica, and amphibole.

Jumillite: Jumilite is leucite lamprophyre (URL-6), consisting primarily of leucite and diopside and secondarily of olivine, alkali feldspar and phlogopite.

Alkali lamprophyres

These lamprophyres are effectively hydrous basanites, all associated with alkali basalts or nepheline syenite/gabbro plutons. Alkaline lamprophyres are generally interpreted as derived from hydrous basanitic or tephritic magmas that developed in crustal dome areas. These include camptonite, monschite, sannaite, quaternite and other rare rocks.

Camptonites: Camptonite is a porphyritic alkaline igneous rock dominated by essential plagioclase and brown amphibole (usually with hornblende and often titanium augite). Plagioclase is found in the dough (URL-6).

Monchiquites: Monchiquite is a porphyritic alkaline igneous rock dominated by essential olivine, titanium augite and brown hornblende (URL-6).

Sannaites: Sannaites are generally similar to camptonites except that they contain alkali feldspar instead of plagioclase (URL-6).

Fourchite: Fourchite is a melanocratic analcime lamprophyre containing abundant augite but no olivine and feldspar.

Other very rare members of this subgroup include:

Mondhaldeite: A type of sannaite composed of equal proportions of plagioclase and alkali feldspar, and secondarily clinopyroxene, amphibole and leucite, in a glassy matrix.

Espichellite: A variety of camptonite containing analcime.

Estratite: A glassy sannaite containing rare olivine phenocrysts, weathered hornblende, and occasional augite in a matrix of augite, titanomagnetite, feldspar, and glass (URL-6).

Heptorite: A haüyne-monchiquite composed of titanium augite, barkevicite, olivine and haüyne phenocrysts in a paste of glass and labradorite laths.

Heumite: A sodalite-sannaite (URL-6) consisting of biotite, hornblende, sanidine and foids.

Giumarrite: A variety of hornblende monchiquite.

Ultramafic lamprophyres

Melilite, perovskite and calcite are characteristic phases. Alnoids are closely related to kimberlites, which can be included in the subgroup. Allylicites are closer to carbonatites than alnoids (URL-6). Ultramafic lamprophyres from local dyke swarms or diatreme clusters are primarily associated with continental rifting and may represent parent magmas for contemporary carbonatite complexes. Their additional occurrence in the oceanic environment, xenolith contents in the mantle, and high mg, Cr, and Ni indicate that many of these are mantle-derived primary magmas formed at depths of melilites and kimberlites (c. 150 km) but at higher CO_2 pressures than melilites (URL-6).

Aillikite: From Aillik Bay, Canada. An ultramafic carbonate-rich lamprophyre (URL-6) consisting of a variety of phenocrysts, including diopsidic pyroxene, olivine, phlogopite and amphiboles

within a matrix of similar minerals that contain at least partial primary carbonate and minor perovskite but no melilite.

Leucites

Leucites are generally porphyritic extrusive or subvolcanic rocks consisting of clinopyroxene (Aegirine, diopside, Titanoaujit) and leucite minerals(Figure 4) (URL-7).

The minerals it contains are plagioclase, k-feldspar, leucite, clinopyroxene, nepheline and olivine. Melilith is not observed in the presence of plagioclase. Phlogopite minerals are commonly seen. Accessory minerals: perovskite, biotite, wadeite, apatite, prideite, magnetite, ilmenite and spinel (URL-7).

Figure 4. Macroscopic views of leucites (URL-7)

Leucite easily decomposes in pre-Tertiary rocks and transforms into analcite, zeolite, and other secondary minerals. It is rarely observed in plutonic rocks and dykes (URL-7).

"Pseudoleucites" are rounded areas composed of feldspar, nepheline, analcite, etc., having the composition, shape, and, in some cases, the external crystal form of leucite; these are probably

pseudomorphs or paramorphs developing from leucite; because this mineral is not stable at ordinary temperatures and can be expected to spontaneously transform into an assemblage of other minerals under suitable conditions. (URL-7).

Rocks containing plutonic leucite are leucite syenite and missourite. The first consists of orthoclase, nepheline, sodalite, diopside, aegirine, biotite, and sphene. Two incidents are known, one in Arkansas and the other in Sutherland, Scotland. The Scottish rock was called borolanite. In both examples, large round spots are visible on the hand samples. They are pseudoleucites and, under the microscope, prove to be composed of orthoclase, nepheline, sodalite and weathering products. These have an external radial arrangement, but their centres have an irregular structure; melanite is an important accessory in both rocks. Missourites with mafic composition contain olivine, leucite, biotite and augite. (URL-7).

Leucite is generally observed in Tertiary lavas. Although leucites contain no quartz, feldspar is often present, although certain groups of leucite lavas are not feldspathic. Many also contain sodalite, nepheline, nosean and hauyne. The much rarer melilite mineral is also seen in some samples (URL-7). The most common ferromagnesian mineral is augite; more basic varieties include olivine. Hornblende and biotite also occur. Melanite is found as well as in leucite syenites. Sodium-rich extrusive leucite with a glassy paste rich in olivine and clinopyroxene is sometimes called ignite (URL-7).

Phonalite

Phonolites are extrusive rocks consisting mainly of alkali feldspar (Anorthoclase and Sanidine), alkali amphiboles, alkali pyroxenes, mafic minerals such as Augite, Biotite and Olivine, and one or more foids. If nepheline is the only foid then the term phonolite alone can be used, but if, for example, leucite is the most abundant foid, the term leucite phonolite should be used. It refers to a stone that makes noise because of its metallic sound when struck

against an unbroken plate; hence the English name clinkstone (URL-1).

Tephrite

Tephrites are extrusive rocks composed mainly of calcic plagioclase, clinopyroxene and foids. Foids normally constitute more than 10% of felsic minerals. The difference between tephrites and basanites is that they do not contain olivine. Tephrite also contains small amounts of alkali feldspar; therefore, with increasing alkali feldspar content, they transform into phonolitic Tephrites and tephritic Phonolites. There are both sodium-rich and potassium-rich Tephrites. Sodium-rich varieties are known from the Canary Islands and Thaiti, and potassium-rich varieties are known from the Roman igneous provinces and Vesuvius. (URL-1).

Basanite

Basanite is an aphanite (fine-grained) igneous rock low in silica and rich in alkali metals (Figure 5). The mineral assemblage in basanite generally consists of olivine with abundant feldspathoids, augite and plagioclase and iron-titanium oxides such as magnetite and ilmenite in lesser amounts; minor alkali feldspar may be present. Olivine and clinopyroxene are common as phenocrysts and within the matrix. Augite contains significantly more titanium, aluminium and sodium than typical tholeiitic basalt. There is no quartz like orthopyroxene and pigeonite (URL-8).

Chemically, basanites are mafic. As seen in the TAS classification diagram, it is low in silica and high in alkaline compared to basalt, which typically contains more SiO_2. Nephelinite is richer in Na_2O plus K_2O than SiO_2 (URL-8).

Figure 5. Macroscopic views of Basanites (URL-8)

Discussion

Alkaline rocks occur in many different tectonic environments and petrological associations and have a wide range of chemical compositions; hence, it is clear that no parent magma can produce all alkaline rocks. Their occurrence on oceanic islands and seamounts suggests that some of the parent magmas may be produced within the mantle and that these magmas may develop in an environment far removed from any possible contamination of continental crust materials. Most petrologists now believe that most alkaline rocks evolved from parent magmas formed by partial melting within the mantle, and fractional crystallization and other differentiation processes can often only emphasize the alkaline tendency already transferred to the parent magma (URL-1).

Alkaline magmatic activity is tightly controlled by releasing volatile-charged magma from the deep mantle source (URL-1). Cracks in the continental lithosphere act as conduit pathways for these magmas, and volatiles and incompatible elements are drained through narrow cracks and rift zones. The second process results in metasomatisms. The composition of the ascending magma is largely controlled by host rock reactions and polybaric fractional

crystallization (URL-1). The heat from the magma causes a gradual increase in partial melting, and a wide variety of different magmas can be produced depending on the composition of the melted materials. It has been suggested that undersaturated alkaline rocks are normally formed within the mantle at a depth of at least 80 km and that the formation of these magmas tends to be triggered by the flow of low-viscosity fluids from the degassing mantle (URL-1).

Conclusion

Alkaline is defined as having a higher alkali concentration than in feldspar alone. It also describes rocks containing significant amounts of foids (nepheline, sodalite, leucite), alkaline pyroxenes, alkaline amphiboles, and melilite. Rocks that contain sufficient or excess silica but lack alumina are grouped as rocks that contain sufficient or excess alumina (enough to saturate the feldspar composition) but lack silica and rocks that are deficient in both silica and alumina according to their feldspar composition. Carbonatites, nephelinites, lamprophyres, phonalites, tephrites and basanites represent alkaline rocks.

REFERENCES

Allington-Jones, L. (2014). "Preserving carbonatite lavas"(PDF). The Geological Curator. 10 (1): 3–8

Brey, G. & Green, D.H. (1975). The role of CO2 in the genesis of olivine melilitite. *Contrib. Mineral. Petrol*. 49, 93–103. https://doi.org/10.1007/bf00373853

Fıtton, J.G. & Upton, B.G.J. (1987). Alkaline Igneous Rocks. *Geological Society Special Publication*, 30, p. 545.

Guilbert, J.M. & Charles F.P. (1986). The Geology of Ore Deposits, Freeman, pp. 188 and 352-361 ISBN 0-7167-1456-6

Kresten, P. (1983). Carbonatite nomenclature, International Journal of Earth Sciences, 72, (1).

Le Bas, M. J. (1999). Sovite and alvikite; two chemically distinct calciocarbonatites C1 and C2, *South African Journal of Geology*,102, 109–121.

Pirajno, F. (2022). The carbonatite story once more and associated REE mineral systems, *Gondwana Research*, 107, 281-295.

Woolley, A.R. & Bailey, D.K. (2012). The crucial role of lithospheric structure in the generation and release of carbonatites: geological evidence. *Mineralogical Magazine*, 76 (2), 259-270.

Yastı, M.A. (2023). Karbonatitler. *MTA Doğal Kaynaklar ve Ekonomi Bülteni*, 35, 17-30.

Yaxley, G.M. & Brey, G.P. (2004). Phase relations of carbonate-bearing eclogite assemblages from 2.5 to 5.5 GPa: implications for petrogenesis of carbonatites. *Contrib. Mineral. Petrol.*, 2004, 146, 606-619.

Zeng, G., Chen, L-H., Hofmann, A.W., Wang, X.J., Liu, J.Q., Yu, X. & Xie, L-W. (2021). Nephelinites in eastern China

originating from the mantle transition zone. *Chemical Geology*, 576, 120276.

URL-1 https://www.alexstrekeisen.it/english/vulc/leucitite.php

URL-2 https://tr.wikipedia.org/wiki/Karbonatit

URL-3 https://geologische-streifzuege.info/karbonatite/

URL-4https://geomapa.lounovicepodblanikem.cz/horniny/57.html

URL-5https://geomapa.lounovicepodblanikem.cz/horniny/70.html

URL-6https://www.alexstrekeisen.it/english/vulc/lamprophyres.php

URL-7 https://en.wikipedia.org/wiki/Leucitite

URL-8 https://en.wikipedia.org/wiki/Basanite

CHAPTER II

The Relationship between Depositional Processes and Biological Productivity of Bituminous Claystones: Ilgin (Konya) Field

Ali SARI[1]
Kamal ISMAYILZADA[2]
Berna YAVUZ PEHLİVANLI[3]
Fuat EROL[4]

Introduction

Ilgın coal field is located in the northwest of Konya province. Operable coal thickness in the field varies between 0,60-21,55 metres. During the coal formation, coal formation was interrupted

[1] Prof.Dr., Ankara University, Eng.Fak.Geo.Eng.Dept., 06830, Gölbaşı, ANKARA,
[2] Postgraduate student, Ankara University, Institute of Science and Technology, 06830, Gölbaşı, ANKARA
[3] Assoc. Prof. Dr., Yozgat Bozok University, Eng.Arch. Faculty. Geological Engineering. Dept. 66200 YOZGAT
[4] Geological Engineer, Turkiye Coal Enterprises (TKI) Corporation General Directorate, Yenimahalle, 06560, ANKARA

from time to time due to the arrival of detrital material to the basin and thickenings occurred in the intersections within the coal. As a matter of fact, coals with less intersections are observed in the northwestern and northeastern parts of the field. In the northern and southern parts of the site, thickening of the interstices and successions with coals have occurred due to the water mobility of the depositional environment. Phytoplankton algal life starts in the lake when the coal formation is completed and the lake starts to deepen slowly. Bituminous claystone sedimentation takes place in this period which is more stagnant.

Bituminous clayey mudstones (claystone and shale) have high phytoplankton algal productivity in the upper water column. There is no O2-rich water circulation in the water table. In other words, they are deposited in water environments rich in reducing H2S, where anoxic conditions prevail. The high organic matter content of bituminous clayey mudstones and the reducing redox conditions of the environment lead to the accumulation of very high amounts of major, trace and rare earth elements in these rocks compared to the surrounding rocks. For this reason, bituminous clayey mudstones are also operated as mineral deposits in the world. These rocks accumulate elements such as U, Th, P, Mo, V, Cu, Zn, Ni, Cr, Co, Pb, Au, and Ag more than the surrounding rocks. Norway (Lipinski et al. 2003), Venezuela (Alberdi-Genolet and Tocco 1999), Mexico (Nameroff et al. 2001), Finland (Loukola-Ruskeeniemi, 1991), United States (Levanthal and Hosterman 1982; Schatzel and Stewort 2002; Paradis 2004), Canada (Moosman et al., 1993). a; Moosman et al. 1993b; Mossman D.J. 1999), it is known that metals such as U, Ag, Se and Te are economically enriched in bituminous rocks. Therefore, it is very important to understand the relationship between the deposition processes and biological productivity of bituminous clayey mudstones.

Alpine tectonism was effective in the formation of Palaeozoic and Mesozoic aged units in the region where the study area is located. In the study area, Mesozoic aged units are unconformably on the Palaeozoic basement (Hüseyinca and Eren

2007). Stratigraphically, the site starts with the Palaeozoic basement. Then, the Mesozoic aged units are unconformably overlain from bottom to top; Bahçecik formation consisting of Lower Triassic aged metacrustics and phyllites; Ertuğrul formation consisting of Lower Triassic aged metacarbonate-metacrustics succession; Kızılören formation consisting of Upper Triassic-Lower Jurassic aged bitumen dolomites; and finally Lorasdağı formation consisting of Lower Jurassic-Lower Cretaceous aged dolomites and calcitic dolomites. These Mesozoic aged units are again covered by Neogene aged formations as angular unconformably. In these units, the Middle Miocene (Middle Serravalian) aged (Karayiğit et al, 1999) Harmanyazı Formation; Upper Miocene-Lower Pliocene aged Ulumuhsine Formation, which starts with conglomerate at the base and consists of limestones at the upper levels; Pliocene aged Sebiller Formation, which generally consists of claystone, conglomerate and different sized materials; Upper Pliocene-Quaternary aged Tekeler Formation, which consists of carbonate and iron cemented limestone and dolomite fragments of different sizes (Hüseyinca and Eren 2007). The Neogene aged formations are overlain by recent alluvium.

Material and Method

The investigation materials in this study are rock samples taken systematically from the bottom to the top of the bituminous claystone levels with very high organic matter content, which are located just above the lignite coals in the field where the coal deposits are located in Ilgın (Konya).

Major and trace element analyses of the bituminous claystone samples were carried out at Ankara University YEBIM laboratory using ICP-OES (Inductively Coupled Plasm-Optic Emission Spectrometry) model device.

Pyrolysis analyses (%TOC analysis) to determine the organic matter content of the rocks were carried out in the laboratories of

TPAO R&D Centre Directorate using the Rock Eval VI device and IFP 160000 standard.

Geochemical Investigations

Clayey mudstones such as seyl and claystones make up about 70 per cent of all sedimentary rocks. They are fine-grained (<0.1 mm) clastic fragments, usually composed of clay minerals (Schieber and Zimmerle, 1998). The sediment forming the seas and claystones varies from river systems, lakes and continental slopes to deep sea basins. These sediments are deposited in very slow moving water environments (Bohacs, 1998). Organic matter-rich bituminous rocks occur not only in stratified, anoxic and/or euxinic deepwater basins such as the Black Sea and the Baltic Sea, but also when the rich biological productivity in the upper water column, resulting from flooding caused by upwelling events, cannot meet the very high oxygen demand that initiates anoxic conditions in the deep water layers. Examples of anoxic conditions in the water column include the Bengal Current on the coastal shelf of south-west Africa (Namibia), and the corresponding south-west African shelf, particularly Walvis Bay, west of Nabibia. Bituminous clayey mudstones also occur in lakes such as Lake Tanganyika and Lake Kivu in the East African rift-lake system. The constituent elements of bituminous clayey mudstones provide important information about the deposition processes of the rocks. Major and trace elements in clayey mudstones generally come from three main sources: detrital, autogenic and biogenic. Each fraction contains an elemental ratio that indicates or signals the extent to which each source contributes to the amount of sediment deposited. Certain elements serve as primary indicators for particular sources. For example, elements such as Ti, Zr, Th, K, Sc, Rb and Al, which are delivered to the sediment in the detrital fraction, are derived from terrestrial sources. The abundance of these elements in the rock is important for organic matter preservation and bituminous claystone deposition. The biogenic fraction consists of elements such as Cu, Ni, Zn, Ca, P, Si (biogenic) and Ba, which are related to

biogeochemical cycles transferred to the sediment by organic matter, carbonate and silica. The abundance of these elements in the rock is used as an indicator of organic productivity. The autogenic fraction is derived from seawater and consists mainly of insoluble oxy-hydroxides, sulphides and elements such as V, Mo and U in organic matter. Mo element abundance, which is one of the indicators of autogenic fraction, is one of the main indicators for the richness of organic matter content in bituminous shales and claystones. In the bituminous claystone samples of Ilgın field, Al-Ti (r: 0,83) and Al-K (r: 0,95) have ***very strong correlations*** (Figure 1). This indicates that Al, Ti and K elements are present in the clay mineral phase, probably as illite minerals (Bowker, 2002).

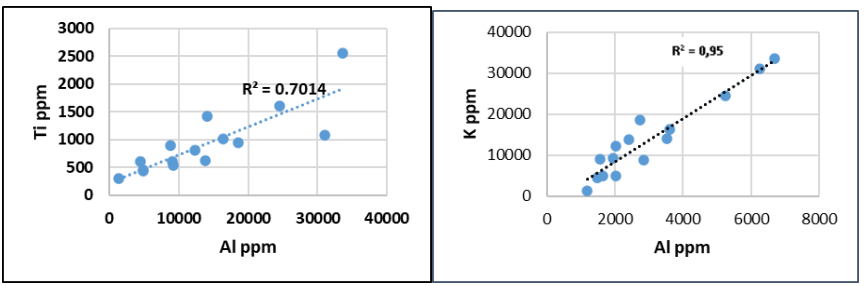

(a) *(b)*

Figure 1.(a) Al-Ti; (b) Al-K correlation relationship

In clayey mudstones, low amounts of quartz (SiO2) and high Al2O3 values indicate that the detrital input to the sedimentary environment has decreased. In the bituminous claystone samples of Ilgın field, there is ***a weak correlation*** (r= 0,084) between Si and Al (Figure 2). When the abundance distributions of Al and Si are analysed, Si values are high while Al values are very low in all samples, indicating that there is a very low amount of detrital input to the environment; the sedimentary environment is a calm water body without energy and the source of Si is biogenic (Figure 3).

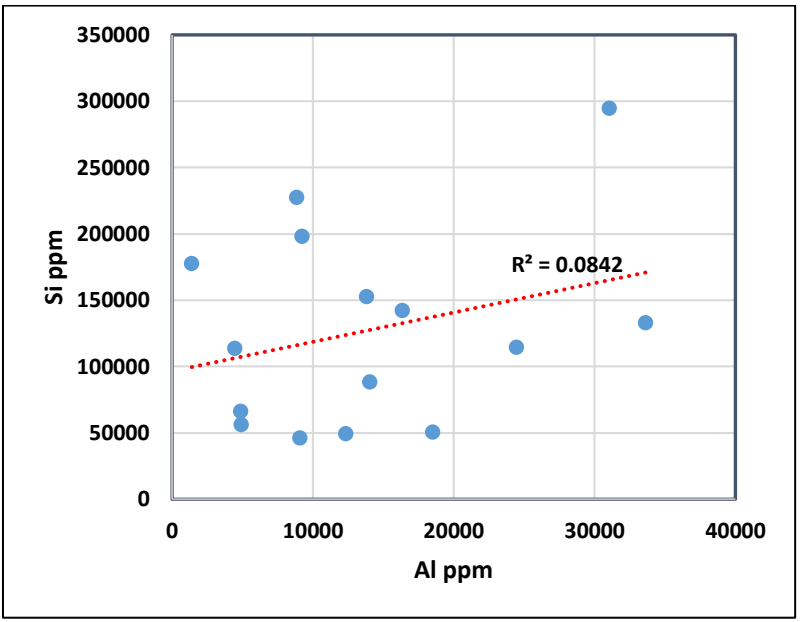

Figure 2. Al-Si correlation relationship

A high Ti/Al ratio reflects the increased loading of fluvial sediments (Murphy et al., 2000). This is because Ti is usually associated with heavy mineral grains. Increased concentrations of Ti relative to Al indicate a higher eolian (wind transport) input (Bertrand et al., 1996). The decrease in the Ti/Al ratio and the increase in the Na/K ratio in the clayey mudstones indicate a decrease in the input of river detritics into the basin. This decrease indicates a relatively quieter depositional period in the basin. If the Ti/Al and Na/K ratios increase at the same time, it may reflect a higher input of volcanic material into the basin. This ratio may also be due to the degradation of basaltic rocks. When the relationship between Ti/Al and Na/K is analyzed in the bituminous claystone samples of the Ilgın field, the decrease in the Ti/Al ratio while the Na/K ratio increases in all samples indicates that the entry of detrital material into the lake basin decreased. In this case, it can be said that there are low energy water conditions and no volcanic material transportation in the basin (Figure 4).

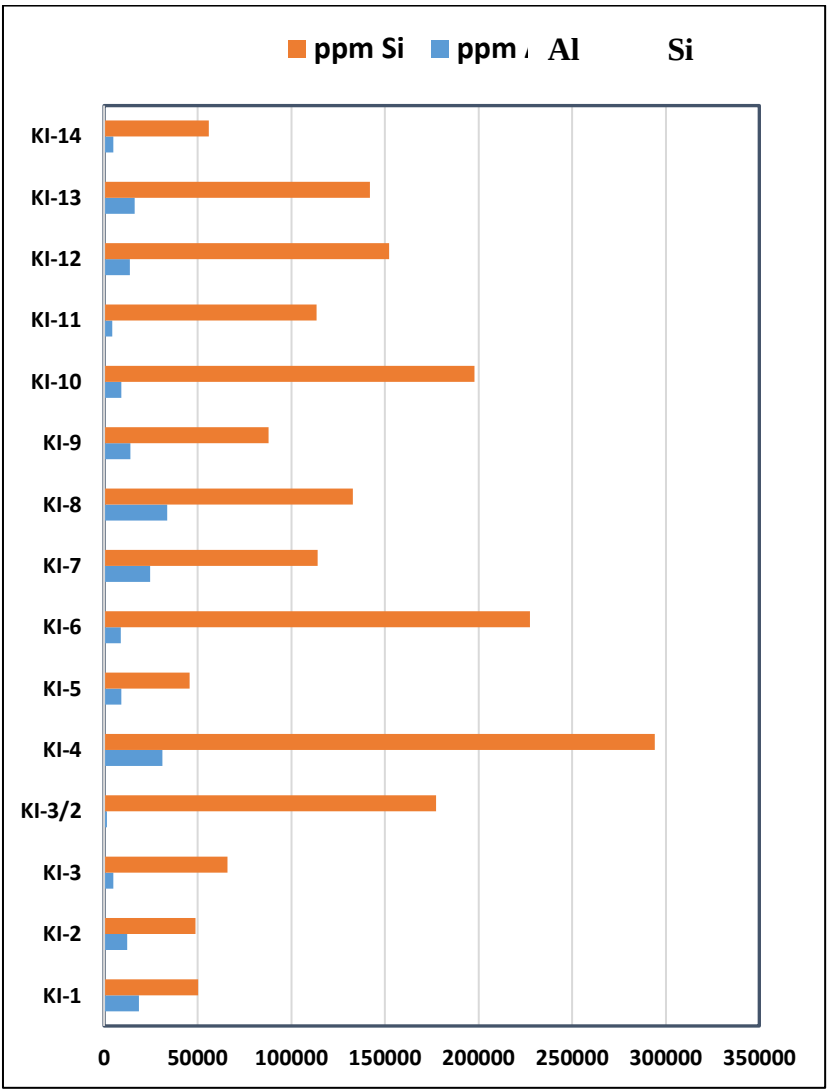

Figure 3. Abundances of Al and Si in bituminous claystone samples of Ilgın field.

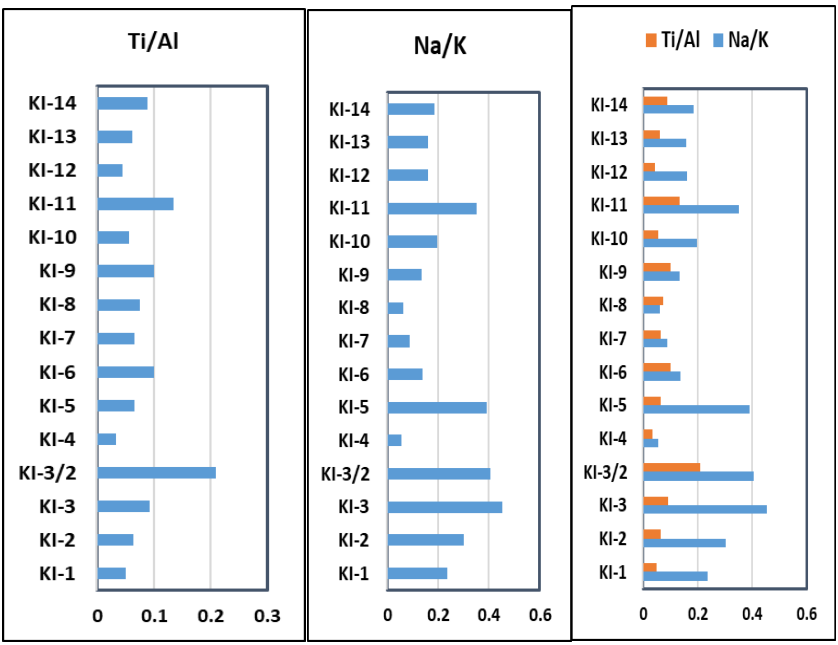

Figure 4. Ti/Al and Na/K relationship in bituminous claystone samples of Ilgın field.

The element Ti is present in the composition of the erosion-resistant mineral rutile (TiO2) from a terrestrial source. The high loading ratio of Ti does not indicate biological participation (Piper and Calvert, 2009). In the absence of biogenic quartz contribution of SiO2 in the sedimentary basin, higher Ti/Al and Na/K ratios and higher Si/Al ratios may be due to higher volcanic or eolian inputs. When the Ti/Al, Na/K and Si/Al ratios in the Ilgın basin are evaluated from this point of view, the fact that Ti/Al and Na/K ratios partially increase while Si/Al ratios show decreasing trends indicates that SiO_2 is a biogenic source rather than detrital/cretaceous. For example, there was no volcanic or eolian input to the Ilgın basin in the Middle Miocene (Middle Serravalian) during the deposition of bituminous claystones. On the other hand, the increase in the Si/Al ratio indicates that there was a decrease in the detrital/sedimentary input, a relative increase in the water level of the lake during this

period, and an increase in the algal productivity of siliceous phytoplankton in the lake environment. In particular, a high Sr/Ca ratio in aquatic environments is typically indicative of a saline environment. In the palaeo-salinity studies carried out on the bituminous claystone samples of the Ilgın field, Sr/Ba (1.32 - 5.24) ratio was 2.870, indicating that the lake water was salty during the deposition of the bituminous claystones. High P and S values support the activity of certain aquatic microorganisms destroying/degrading the organic matter in the sapropel muds at the bottom. In the bituminous claystone samples from the Ilgın field, while the lake water was saline, the fact that P and S values generally follow a compatible trend with each other indicates that sulphate-reducing bacteria destroying organic matter were also active at the lake bottom (Figure 5).

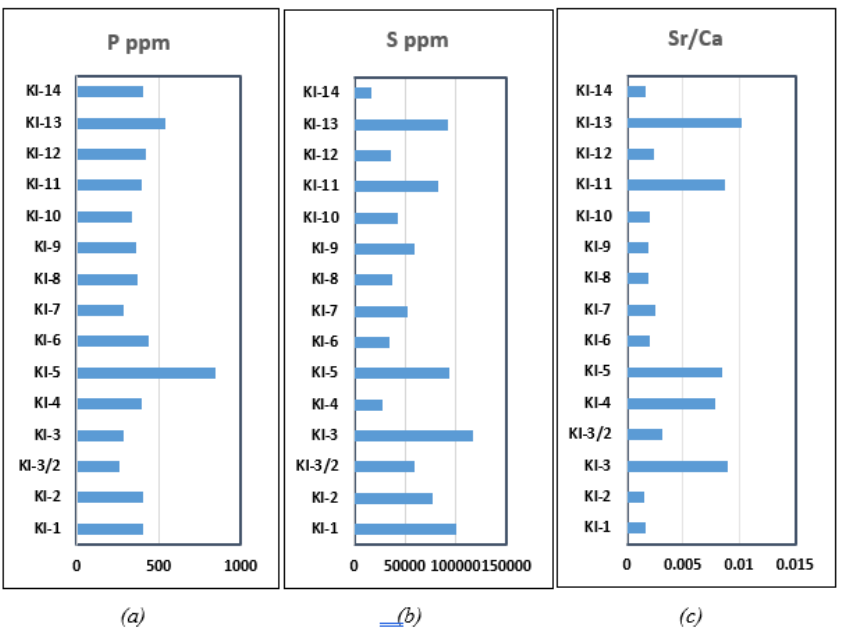

Figure 5. (a) P (ppm) concentration, (b) S (ppm) concentration and (c) Sr/Ca ratio in bituminous claystone samples from Ilgın field.

Discussion

The following issues should be taken into consideration in the storage modelling of bituminous mudstones. These are the lithological and mineralogical properties of the rock under study and the redox conditions of the storage environment. For example, if the grain size of a rock consists of sand and silt size material, this rock was deposited in a high-energy environment and water conditions with abundant oxygen. Such a situation is not important for the formation of bituminous mudstone. If the rock is rich in corbonate minerals (calcite, dolomite etc.), it means that the rock was stored in alkaline waters with plenty of O_2. In this case, if the biological productivity of surface waters is high, the amount of organic matter accumulated at the bottom is generally low due to the low clay content that will envelop and protect the organic matter falling to the bottom. Therefore, there is generally no OM accumulation in limestones. The amount of OM in marls with high carbonate content is lower than in claystones and shales. The high algal productivity at the lake surface and the high organic matter richness in the clayey sediments at the bottom should be considered together. Detailed investigations show that there is a systematic correlation between basic biological productivity and the inorganic matter content of the bottom sediment. Under these conditions, if the biological productivity at the surface is high, the amount of organic matter (OM) preserved at the bottom in the absence of O_2 circulation is expected to be very high. In these conditions, Si/Zr, Cu, Ni and P, which are indicators of biological productivity, and redox-sensitive elements (such as V, Cu, Ni, Co, Mo etc.), Ni/Co ratio and Mo abundance, which are redox indicators of the bottom, are examined. According to Tribovillard et al. (2006), higher Ni/Al and Cu/Al ratios indicate higher water column efficiency. As it is known, there is a very strong relationship between biological productivity at the surface and OM accumulation at the bottom. Therefore, in parallel with the increase in OM, elements such as Cu and Ni, which act as bio nutrients, will have a very strong correlation with %TOC. When analysed from this point of view, Ni/Al, Cu/Al and %TOC have

similar increasing trends in the bituminous claystone samples of Ilgın field (Figure 6).

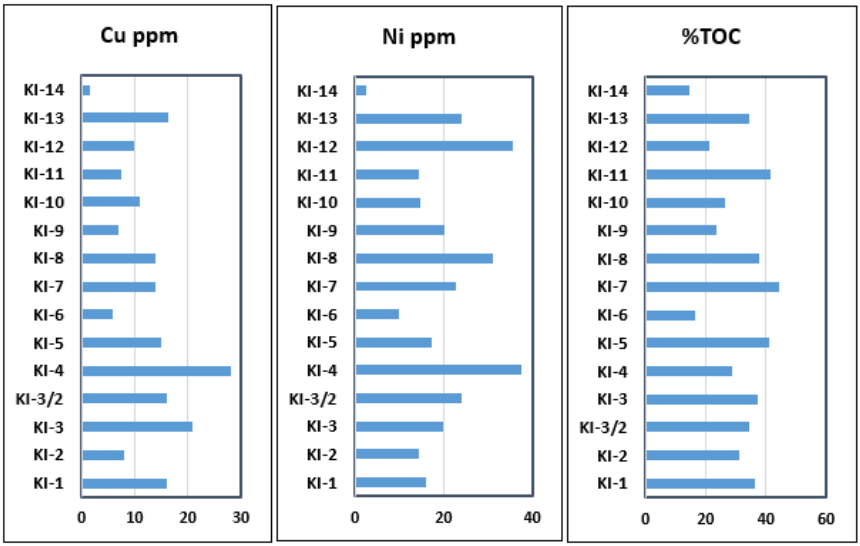

Figure 6. Cu, Ni and %TOC relations in bituminous claystone samples of Ilgın field.

On the other hand, the fact that the Ni/Al and Cu/Al increase trends observed in samples KI-3 and KI-3/2 in Figure 7 are much higher than the other samples indicates that the biological productivity in the precipitation processes of these samples is very high.

When the biological productivity of surface waters is high, the relationship between Si/Zr, which is an indicator of algal productivity, and P, which is a nutrient indicator, will be strong. When the Si/Zr and P relationships are examined in the bituminous claystone samples of Ilgın field, it can be said that the biological productivity of the surface waters is high (Figure 8). The excessive Si trending coinciding with the total P concentration in Figure 8 indicates that the source of Si is biological. Where Si is increased but P is low, Si is associated with quartz of detrital origin. During this

period, detrital input to the basin increases, biological productivity and organic matter conservation decrease.

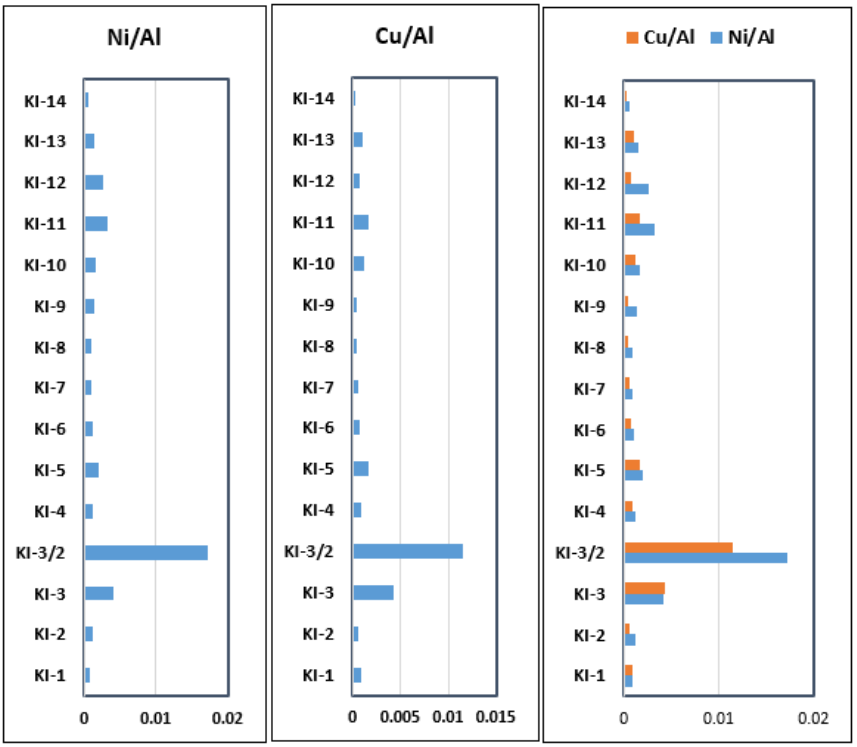

Figure 7. Ni/Al and Cu/Al relationships in bituminous claystone samples from Ilgın field.

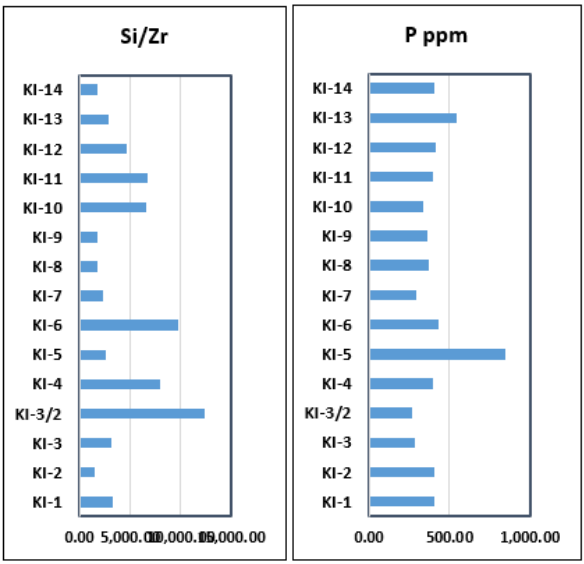

Figure 8. Si/Zr and P relations in bituminous claystone samples of Ilgın field.

In the analysed samples, there is a very strong correlation (r= 0,864) between iron (Fe) and sulphur (S). This indicates that Fe was precipitated in the sulphide phase (Pyrite, FeS_2) and the redox condition was anoxic, H_2S-rich, reducing environment (Figure 9).

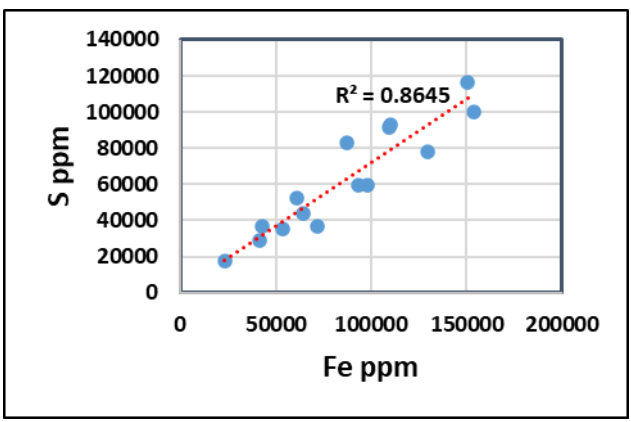

Figure 9. Fe-S correlation relationship

Conclusions

In terms of organic matter accumulation, clayey mudstones under anoxic water bodies are richer than the sediments under oxygenated water bodies. Bituminous clayey mudstones are more abundant in major, trace and trace elements than the surrounding rocks. These elements provide important information about the deposition processes and organic productivity of the rocks. The enrichment of elements from terrestrial sources such as Ti, Zr, Th, K, Sc, Rb and Al in the rock is unfavourable in terms of organic matter richness. On the other hand; elements such as Cu, Ni, Zn, Si (biogenic origin), P and Ba provide important information about biogenic productivity. When the relationship between Ti/Al and Na/K is analysed in the samples examined; the increase in Na/K ratio in all samples while the decrease in Ti/Al ratio indicates that the entry of detritic material into the lake environment decreases. Ni/Al and Cu/Al ratios may be indicators of water column efficiency. There is a very strong relationship between Ni/Al, Cu/Al and %TOC in the bituminous claystone samples of Ilgın field. In the analysed samples; Ti/Al and Na/K ratios increase while Si/Al ratios decrease, indicating that the source of SiO_2 is biogenic. Palaeo-salinity Sr/Ba (1.32 - 5.24) ratio in Ilgın field is 2.870 and it is determined that the lake water was salty during the deposition of bituminous claystones. The fact that high P and S values generally follow a compatible trend with each other indicates that sulphate-reducing bacteria that destroy organic matter are very active in the lake bottom.In conclusion; the amount of organic matter (%TOC, mean: 31,24) in the claystone samples in Ilgın area is quite high.

This indicates that there was no detrital input to the basin during the deposition of bituminous claystones in the Ilgın basin in the Middle Miocene (Middle Serravalian), that the upper water column of the lake, which has acquired saline water characteristics, has a very high productivity of phytoplanktonalgal productivity such as diatoms with Si rods and that the organic matter preservation at the bottom is excellent under anoxic redox conditions.

Acknowledgements

Major and minor element analyses of bituminous claystone samples were performed at Ankara University YEBIM laboratory using ICP-OES (Inductively Coupled Plasm-Optic Emission Spectrometry) model device and we would like to thank them.

REFERENCES

Alberdi-Genolet M, Tocco R., (1999). Tracemetalsandorganicgeochemistry of theMachiquesMember (Aptian–Albian) and La LunaFormation (CenomanianCampanian), Venezuela. *Chem. Geol*. 160:19–38.

Bertrand J., L. Gil de Sola, C. Papaconstantinou, G. Relini et A. Souplet, Coordonnateurs, (1996). Campagne internationale de chalutage démersal en Méditerranée (Medits). Campagne 1995. Rapport final, manuel des protocoles et base de données. Rapport de contrat *CEE-IFREMER-IEO-SIBM-NCMR* (MED/93/020, 018, 006, 004),172 p., 27 p. + annexes.

Bohacs, K.M., (1998).Contrastingexpressions of depositionalsequences in mudrocks from marine to nonmarine environs, in Schieber, J.,Zimmerle, W., and Sethi, P., eds., Mudstone sand Shales, Characteristics at the Basin Scale: Stuttgart, Schweizerbart'sche Verlags buchhandlung vol. 1, , p. 32–77.

Bowker, K.A., (2002). Recent developments of theBarnett Shale play, Fort Worth basin, in B.E Lawand M. Wilson, eds., *Innovative Gas Exploration Concepts Symposium:* Rocky Mountain Association of Geologists and Petroleum Technology Transfer Council, p. 16.

Hüseyinca, M.Y; Eren. Y., (2007). Ilgın (Konya) kuzeyinin stratigrafisi ve tektonik evrimi. *S.Ü. Müh.-Mim. Fak. Derg.,* c.23, s.1-2.

Karayiğit, A.I., Akgün, F.,Gayer, R.A., Temel, A., (1999). Quality, Palynology, And Paleoenvironmental interpretion of The Ilgın Lignite, Turkey. *International Journal of Coal Geology*, 38, 219-236.

Lipinski, M; Warning, B; Brumsack, H,J., (2003).Trace metal signatures of Jurassic/Cret-aceous blackshales from the Norwegian shelf and the Barents Sea. *Palaeogeography, Palaeoclimatology, Palaeoecology*, 190, 459-475.

Levanthal, J.S., and Hosterman, J.W., (1982). Chemical and mineralogical analysis of Devonian blackshale samples from Martin County, Kentucky; Carolland Washington Counties, Ohio; Wise County, Virginia; and Overton County, Tennessee, USA. *Chemical Geology* 37: 237-264.

Mossman, D.J., (1999). Carbonaceoussubstances in mineral deposits: implications for geochemical exploration. *Journal of Geochemical Exploration*, 66: 241-247.

Mossman, D.J., Goodarzi, F., and Gentzis, T., (1993a). Characterization of insoluble organic matter from the Lower Proterozoic Huronian Super group, Elliot Lake, Ontario. *Precambrian, Research,* 61: 279-293.

Mossman, D.J., Naggy, B., andDavis, D.W., (1993b). Hydrothermal alteration of organic matter in uranium ores, Elliot Lake, Canada: Implications for selected organic-rich deposits. *Geochemica et Cosmochemica Acta*, 57: 3251-3259.

Murphy, A.E., Sageman, B.B., Hollander, D.J., (2000). Eutrophication by decoupling of the marine biogeochemical cycles of C, N, and P: A mechanism for the Late Devonian mass extinction. *Geology*, 28, 427–430.

Nameroff, T.J, Balutrier, L.S and Murray, J.W., (2001). Suboxictrace metal geochemistry in the Eastern Tropical North Pacific. *Geochemica et Cosmochemica Acta* 66: 1139-1158.

Paradis, S., (2004). Fluid inclusion and isotope evidence for the origin of the Upton Ba-Zn-Pb deposit, QuebecAppalachians, Canada. *Economic Geology*, 99: 807-817.

Loukola-Ruskeeniemi, K.,1991. Geochemicalevidenceforthehydrothermalorigin of sulphur, basemetalsandgold in Proterozoicmetamorphosedblackshales, KainuuandOutokumpuareas,
Finland.MineraliumDepositavolume 26, pages152–164.

Piper, D.Z., and Calvert, S.E., (2009). A marine biogeochemical perspective on blackshale deposition. *Earth-Sci. Rev.*, 95, 63–96.

Schatzel, S.J., and Stewart, B.W., (2002). Rare earth element source sand modification in the Lower Kittanning coal bed, Pennsylvania: implications for the origin of coal mineral matter and rare earth element exposure in underground mines. *International Journal of Coal Geology* 54: 223-251.

Schieber, J., and Zimmerle, W., (1998). The history and promise of shale research. In: J.Schieber, W. Zimmerle, and P. Sethi (editors), Shale sand Mudstones (vol. 1): Basin Studies, *Sedimentology and Paleontology*, Schweizerbart'sche Verlagsbuchhandlung, Stuttgart, p. 1-10.

Tribovillard, N., Algeo, T. J., Lyons, T. and Riboulleau, A., (2006). Trace metals as paleoredox and paleoproductivity proxies: An update. *Chemical Geology*, 232. 12-32.

CHAPTER III

The benefits of utilising mathematical modeling in the field of rock geochemistry studies

Cihan YALÇIN[1]
Abdullah SAR[2]
Mehmet Ali ERTÜRK[3]

Introduction

Mathematical models play a vital role in comprehending compression processes, system design, and performance evaluation. The integration of this approach with computer hardware and numerical methodology provides benefits such as reduced time and cost, extensive output, and convenience for parametric research and

[1] Dr.; Ministry of Industry and Technology, Worldbank PIU. cihan.yalcin@sanayi.gov.tr ORCID No: 0000-0002-0510-2992
[2] Dr. Arş. Gör.; Fırat University,Engineering Faculty, asar@firat.edu.tr ORCID No: 0000-0002-9752-7807
[3] Dr. Öğr. Üyesi; Fırat University, Engineering Faculty, erturkmae@gmail.com ORCID No: 0000-0003-1197-9202

optimization analysis (He et al., 2009). Obtaining certain parameters through experimental methods can be challenging, but mathematical models offer comparable fundamental physics for different installations. Consequently, the development of accurate mathematical models for ejectors has become a focal point in numerous research endeavors. A multitude of mathematical models have been created and utilized to examine, enhance, and create ejectors (He et al., 2009). This article analyzes the advancements achieved in the mathematical modeling of ejectors and provides a concise overview of notable research conducted in this field.

Geochemical analyses and other data are essential for comprehending the geodynamic histories of Earth and the various local and global processes that occur (Keller & Schoene, 2018). The proliferation of global data collection is attributed to the widespread accessibility of techniques such as X-ray fluorescence and ICP-MS (Gard et al., 2019). Nevertheless, as a result of the exponential growth in recent publications and the substantial division of journals, locating and compiling this data can be arduous and time-consuming (Keller & Schoene, 2018). Ensuring the accessibility of this information is crucial for future studies to develop more reliable models and constrained analyses (Iwamori & Nakamura, 2015). Geochemical compilations have been utilized in diverse investigations, encompassing crustal magma reservoirs, alterations in mantle dynamics, regional and global tectonic chronicles, and the interrelations between life and the Earth (Carbotte et al., 2013). These findings have significant ramifications for the management of the environment, land utilization, and the development of mineral resources (Cox et al., 2018; Gard et al., 2019).

The analysis of geochemical data is crucial for mineral exploration and whole-rock geochemistry because it has a substantial influence on the distribution of fluids, hydrothermal processes, and the structure of the Earth (Cheng et al., 2000; Carranza, 2008; Ghezelbash et al., 2020a, 2020b; Akbari et al., 2023). Through the examination of geospatial data, it is possible to identify unusual trends in geochemical populations, which can aid in

the identification of untapped mineral resources and enhance our comprehension of geological phenomena (Vriend et al., 1988; Bigdeli et al., 2022). Choosing suitable methods to classify geochemical data into meaningful categories is essential during the initial phases of mineral exploration. It is crucial to differentiate between background and anomalous classes, and unsupervised clustering methods such as K-means, K-medoids, and fuzzy c-means are frequently employed for this purpose (Daviran et al., 2020).

Geochemical analyses, including major oxides, trace elements, and rare earth elements, provide crucial indicators for determining geological structure and making informed decisions. To interpret this data, diagrams are created that incorporate intricate mathematical elements. Like in all professional fields, the use of mathematical models to create diagrams and interpret geological structures is a widely applicable method in decision-making processes. Additionally, there exist simplified models, such as the semi-empirical model, which are designed to facilitate calculations. Furthermore, mathematical modeling is a highly efficient method for establishing a correlation between experimental results and empirical performance by utilizing extensive datasets. This study will examine the benefits of employing mathematical modeling to analyze rock chemistry data for geological modeling.

Mathematical model

Mathematical modeling is an essential tool for articulating scientific knowledge, which can result in new findings and questioning established beliefs (Forrester, 1961). The process entails scrutinizing, assessing, and confirming mathematical models. Forrester underscores the importance of a mathematical model's sustainability for a particular objective. Shaeffer's methodological approach comprises the examination of models, algorithms, data evaluation, sensitivity analysis, validation studies, and code comparison studies. Hamilton's (1991) extensive compilation of publications on model validation is also remarkable (Tedeschi, 2006).

Assessing the precision and accuracy of forecasts, developing confidence, or permitting alternative models relies heavily on evaluating the sufficiency of the model (Tedeschi, 2006). Forrester (1961) highlights the importance of mathematical models' validity, whereas Shaeffer (1980) devised a methodical framework comprising six tasks: scrutinizing the model, examining the algorithm, evaluating the data, conducting sensitivity analysis, performing validation experiments, and comparing codes.

Mathematical modeling is an essential component of engineering that uses mathematics to describe and analyze real-world interactions and dynamics. It has a crucial function in domains such as the environment and industry, with the possibility of making significant contributions in multiple areas. The success of mathematical modeling is credited to the rapid advancement of scientific computation, which allows for the conversion of mathematical models into algorithms suitable for high-performance computers. Emerging fields such as information and communication technology, bioengineering, financial engineering, and geology engineering are employing mathematical modeling to effectively handle the intricacies of technology and enhance the speed of innovation (Parolini and Quarteroni).

Mathematical modeling involves the representation of a system or process using mathematical equations and formulas. It enables the mathematical representation of real-world scenarios. The choice of mathematical modeling methods can vary depending on the specific system or process being considered. Mathematical modeling offers benefits in enhancing comprehension, forecasting, and optimization. Mathematical modeling is an effective tool that aids in comprehending and addressing real-life scenarios.

Utilizing the Mathematical Model

Mathematical modeling is applied in scientific studies through various methods. Below are several approaches for implementing mathematical modeling in scientific research:

1. Establishing the Theoretical Framework: Before commencing the study, it is imperative to comprehend the phenomenon or system under investigation and ascertain the fundamental principles that will be employed in the model. The process commences with a comprehensive literature review, followed by a meticulous examination of established scientific theories and a rigorous analysis of the available data.

2. Establishing Modeling Goals and Parameters: The objective of modeling is to ascertain the variables, processes, or interactions that should be incorporated into the model. Additionally, it is necessary to establish the parameters of the model and ascertain their values, whether they are already known or estimated.

3. Formation of Mathematical Equations: Mathematical equations are formulated by the established theoretical framework and objectives. These equations represent fundamental relationships that elucidate the phenomenon or process.

4. Data Collection and Analysis: The necessary data for constructing and verifying the model are gathered and scrutinized. This step is crucial for determining the parameters of the model or evaluating the model's accuracy in representing the real data.

5. Model Development and Adaptation: Typically, the initial model constructed is a rudimentary iteration. During this phase, endeavors are undertaken to enhance the model by increasing its complexity or adjusting it with fresh data.

6. Simulation and Analysis: The model is utilized to conduct simulations or calculations and evaluate its behavior under different circumstances. This can be utilized to forecast forthcoming occurrences or alterations.

7. Validation and Evaluation: The model that has been developed must undergo validation by comparing its performance with actual data. The evaluation of the model includes assessing its level of fit, predictive capacity, and accuracy.

8. Interpretation and Reporting of Results: The interpretation and reporting of results involve analyzing the outcomes of the modeling study and presenting the findings rigorously and scientifically. This can be accomplished through scientific papers, reports, or presentations.

These steps encompass the fundamental procedures employed for the implementation of mathematical modeling in scientific investigations as a whole. The procedural variations may arise in interdisciplinary studies or across various disciplines, yet the fundamental principles remain analogous.

An investigation into the mathematical modeling of rock geochemistry

Rock geochemistry is a scientific discipline that focuses on analyzing the makeup, origin, and development of rocks. Rocks are cohesive geological substances that result from the amalgamation of minerals or mineral particles. Rock chemistry enables us to comprehend the chemical mechanisms accountable for the genesis and development of rocks. Rock chemistry is a scientific discipline that pertains to the study of rocks and their chemical properties, encompassing fields such as geology, petrology, mineralogy, and chemistry. Gaining knowledge about the structure, origin, and development of rocks enables us to acquire insights into the historical and transformative processes of the Earth.

These studies employ mathematical modeling to elucidate the composition and characteristics of rocks, comprehend the processes of rock formation, and ascertain the genesis of rocks.

The classification of mathematical models used in rock geochemistry studies is as follows:

- Geochemical models are utilized to elucidate the compositions and characteristics of rocks. Chemical equilibrium models, such as those used in geology, explain the chemical equilibrium that governs the composition of rocks. Nevertheless,

their purpose is to ascertain mineralization, the configuration of rocks, the process by which rocks are formed, the tectonic setting, and the chemical degradation and alteration occurring in a particular area.

- Rock formation models elucidate the processes involved in the creation of rocks. Models of magmatism elucidate the process by which igneous rocks are formed. Additionally, it addresses significant inquiries about geodynamic evolution, rock composition, and geological structure.

- Rock genesis models: These models are utilized to ascertain the provenance of rocks. Isotope geochemistry models are utilized to ascertain the provenance of rocks, as an illustration.

Mathematical modeling provides several benefits in the field of rock geochemistry studies:

1. Simplifies Complexity: Rock geochemistry focuses on the interplay of numerous factors. Mathematical models can simplify this intricacy, facilitating the analysis of complex relationships.

2. Predictive Capacity: Mathematical models can aid in forecasting rock formation and alteration processes. They can replicate the impacts on the composition or characteristics of rocks under specific circumstances.

3. Data Analysis and Interpretation: Mathematical models can be employed in rock geochemistry studies to analyze large data sets and extract valuable insights from the data.

4. Cost Reduction and Experiment Streamlining: Mathematical models offer a cost-effective alternative to expensive field studies and laboratory experiments. They allow for virtual experiments and the prediction of outcomes under specific conditions.

5. Hypothesis Testing: Mathematical models can be employed to evaluate specific hypotheses and determine the precision or soundness of those hypotheses. This can facilitate the

testing of hypotheses or conjectures regarding the formation of rocks.

6. Auxiliary Tool: Mathematical models can assist in supporting or elucidating data acquired through laboratory or field studies. By doing so, they can aid in comprehending the observed phenomena.

Nevertheless, the utilization of mathematical models may encounter certain constraints. Models may lack a comprehensive representation of the intricate nature of the real world or may rely on specific assumptions that, in certain instances, may not accurately depict reality. Hence, both experimental studies and modeling hold significant importance. Optimally, a comprehensive methodology that integrates modeling techniques bolstered by empirical data can yield the most dependable outcomes.

Rock geochemistry can be analyzed using chemical methods, which then allows the data to be mathematically modeled and represented using various diagrams, formulas, and distinct mathematical expressions. These mathematical models enable us to visualize the outcomes using expressions that accurately represent the distinct features of each analysis. Moreover, diverse graphs, maps, and simulations can be created utilizing distinct methodologies and approaches.

The chemical analysis data can be mathematically represented using various equations or mathematical expressions, thanks to the application of mathematical modeling. These expressions are applicable for elucidating the dynamics and interconnections of geochemical processes. Mathematical models can provide comprehension of intricate processes, such as the distribution of elements or the evolution of their reactions over time.

Moreover, these data and models can be utilized to generate diverse graphs, maps, and simulations. For instance, geochemical data can be utilized to generate graphs illustrating the distribution of elements. Additionally, geographic information systems (GIS) can

be employed to produce maps displaying geochemical properties. Furthermore, laboratory experiments can be validated by conducting simulations.

Mathematical modelling facilitates a more profound comprehension and graphical depiction of the data acquired in the realm of rock geochemistry. Thus, geochemical analyses yield comprehensible results and serve as a crucial tool for comprehending and visualizing geological processes.

Discussion

The application of mathematical modeling in the study of rock geochemistry provides numerous invaluable advantages, greatly improving our comprehension and investigation of geological processes. This discussion will explore the numerous benefits that arise from incorporating mathematical models into studies of rock geochemistry.

Mathematical modeling is a potent tool for interpreting and predicting intricate geological phenomena. These models allow researchers to replicate complex processes like mineral reactions, element migration, and geochemical cycles, offering an understanding into the fundamental mechanisms that govern these phenomena. Through the application of mathematical equations and simulations, scientists can gain a visual understanding of the progression of geological systems over time. This enables them to make predictions about future changes or behaviors.

Moreover, the incorporation of mathematical models enables the assimilation and comprehension of various datasets. Rock geochemistry entails the examination of data obtained from diverse sources, such as field observations, laboratory experiments, and remote sensing. Mathematical models offer a structure to combine these different datasets, allowing researchers to make comprehensive conclusions and find connections between various parameters.

Another notable advantage is the enhancement of resource exploration and extraction through optimization. Mathematical models are utilized in industries such as mining and oil exploration to facilitate the identification of potential mineral or hydrocarbon deposits, the estimation of their size and distribution, and the comprehension of their chemical compositions. This optimization results in the implementation of more efficient and sustainable practices for managing resources, thereby reducing environmental impacts while maximizing resource extraction.

Furthermore, the use of mathematical modeling enables the development and implementation of strategies for evaluating and addressing environmental issues. Through the simulation of various scenarios, these models facilitate the assessment of the ecological consequences associated with geological activities, such as mining or groundwater pollution. They aid in formulating strategies to alleviate pollution, forecast the dissemination of pollutants, and pinpoint susceptible regions, thereby enhancing the efficacy of environmental management and conservation endeavors.

Moreover, these models function as a foundation for conducting hypothesis testing and verification. Scientists can evaluate theoretical frameworks by conducting simulations and comparing them with empirical data. This process allows them to validate hypotheses and enhance scientific theories in the field of rock geochemistry.

The integration of mathematical modeling is crucial for making well-informed decisions across different industries. These models offer valuable insights grounded in scientific evidence, allowing stakeholders and policymakers to make well-informed decisions in various fields such as industrial applications, environmental policies, and hazard management.

Gard et al. (2019) developed a comprehensive worldwide geochemical database by merging existing datasets and adding new ones as supplements. They created a system for naming, calculated geochemical indicators, and made estimates of physical properties.

Esmailzadeh et al. (2023) devised a novel MIP (Mixed Integer Programming) model to optimize the coordination of open-pit and underground mining activities. They employed an allocation-based scheduling strategy to maximize the utilization of Open-Pit Waste Rock (OPWR) while minimizing the expenses associated with waste rock haulage and mine closure.

Shirazi et al. (2023) devised an extensive geochemical modeling (mathematical modeling) method to study copper mineralization in the Sahlabad region of Birjand, East Iran. They employed inductively coupled plasma mass spectrometry and machine learning techniques to examine 709 stream sediment samples.

Sahu & Jhariya (2023) examined the present state of the aquifer and levels of stress, with the goal of constructing a flow model to comprehend the direction of groundwater flow, predict future conditions, and comprehend patterns of SO_4 concentration. A 3D mathematical model was created to accurately mimic the flow of groundwater and the concentration of sulfate in the Tantaria watershed in Chhattisgarh, India.

Conclusion

The utilization of mathematical modeling in rock geochemistry studies provides several advantages, such as the ability to make predictions, integrate data, optimize resources, assess the environment, test hypotheses, and support decision-making. The progress of technology enables the expansion of integration, resulting in enhanced knowledge, more precise predictions, and a more profound comprehension of Earth's geological processes. Furthermore, it impacts sectors such as mining, energy exploration, and environmental management by enhancing resource exploration, improving extraction methods, and assisting in environmental remediation and hazard mitigation. Mathematical models play a crucial role in facilitating well-informed decision-making, allowing stakeholders and policymakers to effectively address intricate

geological obstacles by relying on evidence-based guidance. Virtual experimentation allows for hypothesis validation and reduces reliance on costly fieldwork by providing a cost-effective alternative.

REFERENCES

Akbari, S., Ramazi, H., Ghezelbash, R., & Maghsoudi, A., (2020). Geoelectrical integrated models for determining the geometry of karstic cavities in the Zarrinabad area, west of Iran: combination of fuzzy logic, CA fractal model and hybrid AHP-TOPSIS procedure. *Carbonates and Evaporites* 35, 1–16.

Bigdeli, A., Maghsoudi, A., & Ghezelbash, R., (2022). Application of self-organizing map (SOM) and K-means clustering algorithms for portraying geochemical anomaly patterns in Moalleman district. NE Iran. *J. Geochem. Explor*. 233, 106923.

Carbotte, S. M., Marjanovic, M., Carton, H., Mutter, J. C., Canales, J. P., Nedimovic, M. R., Han, S., & Perfit, M. R. (2013). Fine-scale segmentation of the crustal magma reservoir beneath the East Pacific Rise, *Nat. Geosci., 6,* 866–870, https://doi.org/10.1038/ngeo1933.

Carranza, E.J.M. (2008). Geochemical Anomaly and Mineral Prospectivity Mapping in GIS, vol. 11. *Elsevier*.

Cheng, Q., Xu, Y., Grunsky, E., (2000). Integrated spatial and spectrum method for geochemical anomaly separation. *Nat. Resour. Res*. 9 (1), 43–52.

Cox, G. M., Lyons, T. W., Mitchell, R. N., Hasterok, D., & Gard, M. (2018). Linking the rise of atmospheric oxygen to growth in the continental phosphorus inventory, *Earth Planet. Sci. Lett*., 489, 28– 36, https://doi.org/10.1016/j.epsl.2018.02.016.

Daviran, M., Maghsoudi, A., Cohen, D.R., Ghezelbash, R., & Yilmaz, H., (2020). Assessment of various fuzzy c-mean clustering validation indices for mapping mineral prospectivity: combination of multifractal geochemical model and mineralization processes. *Nat. Resour. Res*. 29 (1), 229–246.

Esmailzadeh, S., Bakhtavar, E., Mokhtarian-Asl, M., Sadiq, R., & Hewage, K. (2023). Mathematical modelling of waste rock management through incorporating open-pit waste rocks in

underground stope filling: An environmental approach, *Resources Policy*, Volume 85, Part B, 103885, ISSN 0301-4207, https://doi.org/10.1016/j.resourpol.2023.103885

Gard, M., Hasterok, D., & Halpin, J. (2019). *Global wholerock geochemical database compilation (Version 1.0.0)*, https://doi.org/10.5281/zenodo.2592823.

Ghezelbash, R., Maghsoudi, A., & Carranza, E.J.M., (2020a). Optimization of geochemical anomaly detection using a novel genetic K-means clustering (GKMC) algorithm. *Comput. Geosci*. 134, 104335.

Ghezelbash, R., Maghsoudi, A., & Carranza, E.J.M., (2020b). Sensitivity analysis of prospectivity modeling to evidence maps: enhancing success of targeting for epithermal gold, Takab district, NW Iran. *Ore Geol. Rev.* 120, 103394.

He, S., Li, Y., & Wang, R.Z. (2009). Progress of mathematical modeling on ejectors, *Renewable and Sustainable Energy Reviews*, Volume 13, Issue 8, 2009, Pages 1760-1780, ISSN 1364-0321, https://doi.org/10.1016/j.rser.2008.09.032.

Iwamori, H. & Nakamura, H. (2015). Isotopic heterogeneity of oceanic, arc and continental basalts and its implications for mantle dynamics, *Gondwana Res.*, 27, 1131–1152, https://doi.org/10.1016/j.gr.2014.09.003.

Keller, B. & Schoene, B. (2018). Plate tectonics and continental basaltic geochemistry throughout Earth history, Earth Planet. *Sci. Lett.*, 481, 290–304, https://doi.org/10.1016/j.epsl.2017.10.031.

Parolini, N., & Quarteroni, A. (2005). Mathematical models and numerical simulations for the America's Cup, *Comp. Meth. Appl. Mech. Eng.*, 173, 1001–1026.

Sahu, K.S., & Jhariya, D.C. (2023). 3D-Mathematical model to simulate groundwater flow and sulfate concentration in Tantaria

watershed, Bemetara district, Chhattisgarh, India. Environment, *Development and Sustainability*, 25:1667–1683

Shirazi, A., Hezarkhani, A., Shirazy, A., & Pour, A.B. (2023). Geochemical Modeling of Copper Mineralization Using Geostatistical and Machine Learning Algorithms in the Sahlabad Area, Iran. *Minerals*, 13, 1133. https://doi.org/10.3390/min13091133.

Tedeschi, L.O. (2006). Assessment of the adequacy of mathematical models. *Agricultural Systems*, 89, 225–247.

Vriend, S.P., Van Gaans, P.F.M., Middelburg, J., & De Nijs, A., (1988). The application of fuzzy c-means cluster analysis and non-linear mapping to geochemical datasets: examples from Portugal. *Appl. Geochem*. 3 (2), 213–224.

CHAPTER IV

Advantages of Applying Machine Learning Theory in the Investigation of Mineral Deposits

Cihan YALÇIN[1]

Introduction

Machine learning algorithms are now essential in mineral exploration as they aid in comprehending and streamlining the mineralization process (Singer and Kouda, 1999; Kreuzer et al., 2008; Chen and Zhao, 2011; Liu et al., 2011; Ford and Hart, 2013; Ghezelbash et al., 2019; Davies et al., 2020; Kreuzer et al., 2020; Parsa and Carranza, 2021; Yousefi et al., 2021). These algorithms are employed for the analysis of extensive datasets, including geological data obtained from volcanic rocks, protoliths derived

[1] Dr.; Ministry of Industry and Technology, Worldbank PIU. cihan.yalcin@sanayi.gov.tr ORCID No: 0000-0002-0510-2992

from metamorphic rocks, and areas with potential for mineral prospecting (Petrelli and Perugini, 2016; Ueki et al., 2018; Ge et al., 2021; Zhong et al., 2021a). Nevertheless, these techniques frequently prove to be excessively intricate to be executed flawlessly, thereby posing challenges in extracting mineralization criteria from intricate exploration data (Jessell et al., 2014; Witherly, 2014; Qin and Liu, 2018; Liu and Qin, 2019).

To tackle this challenge, computational modeling, which includes geometric modeling, geodynamic simulation, and statistical and machine learning (ML) modeling, has emerged as a strong supplement to conventional methods (Gregory et al., 2019; Saha et al., 2021). Supervised machine learning algorithms, such as Random Forest (RF), XGBoost, lightGBM, support vector machine (SVM), and artificial neural networks (ANN), have been employed to enhance the precision and dependability of classifications (Zhong et al., 2021a; Wang et al., 2021a). Nevertheless, the classification model produced by these algorithms may seem opaque, posing challenges in establishing connections between geological and/or geochemical interpretation and the characteristics of the original data and predicted results (Li et al., 2023).

Various techniques, including RF's feature importance based on the Gini index, incremental feature addition, and Shapley Additive explanations, have been utilized to assess the relative significance of elements (Louppe, 2014). These methods enhance the comprehension of mineral geochemistry across diverse geological contexts. In general, machine learning can transform mineral exploration by offering more precise and dependable categorizations of mineralization and geological characteristics (Gregory et al., 2019; Saha et al., 2021; Zhong et al., 2021b).

The processing of geochemical data has gained significant importance in recent years to detect anomalies associated with mineralization (Qin and Liu, 2018; Liu and Qin, 2019). Supervised machine learning algorithms are being explored as a promising technology for analyzing geoscience data. This includes tasks such

as distinguishing different tectonic settings, identifying the original rock types, and determining the origin of minerals like apatite, pyrite, magnetite, biotite, quartz, and zircon (Gregory et al., 2019; Huang et al., 2019; O'Sullivan et al., 2020; Saha et al., 2021; Wang et al., 2021b; Zhong et al., 2021b; Zheng et al., 2022; Hu et al., 2022).

The process of discovering and exploring mineral deposits is intricately complex, and the application of machine learning theory can yield numerous advantages in this domain. The utilization of machine learning is progressively prevalent in the investigation of mineral deposits. This enables mining companies to generate more precise forecasts that are more efficient and impactful in comparison to conventional approaches. This study aims to elucidate the impact of this technique on mineral exploration.

Machine Learning (ML)

Artificial intelligence (AI) is a discipline that concentrates on the advancement of computer systems with the ability to carry out tasks that necessitate human intelligence, including visual perception, speech recognition, decision-making, and language translation (Russell and Norvig 2021). At first, AI depended on manually created rules to encode established connections, processes, and decision-making logic into intelligent systems. Nevertheless, the emergence of new programming frameworks, the abundance of data, and the advancement in computing power have led to a growing trend of constructing analytical models through machine learning (ML) (Brynjolfsson and McAfee 2017; Goodfellow et al. 2016). This approach alleviates humans from the task of converting their knowledge into machine-readable formats, resulting in a more streamlined development process for intelligent systems (Ula, 2020). Machine learning and deep learning are prevalent artificial intelligence methodologies, categorized into generative models and discriminative models (Gupta, 2020). AI, or Artificial Intelligence, is a branch of the IT sector that focuses on the development of

machines that can mimic human behavior. Its primary objective is to create intelligent computer programs.

Machine learning (ML) is a method that trains machines to effectively process data, particularly in cases where the information is challenging to interpret. Due to the plethora of accessible datasets, there is a growing demand for machine learning (ML), which is being employed across diverse industries to extract pertinent information. Machine learning utilizes a range of algorithms to address data-related issues, with no universally superior algorithm that suits all scenarios. Diverse methodologies are employed to surmount the obstacles posed by extensive data sets (Mahesh, 2020). Simultaneously, the progress in machine learning has driven the emergence of intelligent systems possessing cognitive abilities similar to humans. These systems have become prevalent in both our professional and personal lives, influencing various aspects of networked interactions in electronic markets (Fischer et al., 2020).

Machine learning (ML) refers to a computer program that enhances its performance by gaining experience in specific tasks and metrics (Jordan and Mitchell 2015). It uses iterative algorithms to automate the process of constructing analytical models for cognitive tasks such as object detection or analysis, based on problem-specific training data. Machine learning is especially advantageous for tasks involving data with a large number of dimensions, such as classification, regression, and clustering. It enhances the ability to generate dependable and consistent decisions by acquiring knowledge from past calculations and identifying patterns from extensive databases. ML algorithms have proven effective in diverse domains such as mineral deposits, image processing, social analysis, speech and language translation, among others. There is a wide range of machine learning algorithms that can be used for learning (Bishop, 2006).

The mining industry, like many other sectors, is increasingly adopting machine learning, and this adoption is projected to persist in the foreseeable future. Greater implementation of this technology

could facilitate the mining industry to become more efficient and lucrative. By considering multiple criteria in decision-making processes and mineral exploration studies, one can achieve efficient, environmentally friendly, and outcome-focused outcomes.

Mineral Exploration

Mineral exploration involves the systematic investigation of underground mineral resources to assess their economic viability for exploitation. Geological, geophysical, and satellite data are extensively utilized in these studies.

Geological data form the foundation of mineral exploration. This dataset offers insights into the genesis, composition, and development of the Earth's crust. Geological data can be acquired through field observations, geological maps, geochemistry, isotopes, fluid inclusions, geological reports, and other geological sources.

Geological data can be utilized in mineral exploration for the subsequent objectives:

1. To ascertain the geological conditions under which mineral resources are formed

2. To assess the economic viability of mineral resources

3. To ascertain the spatial allocation of mineral resources

Geophysical data refers to techniques employed to examine the physical characteristics of the underground. These methods enable the determination of the subsurface's structure and properties by measuring the density, permeability, electrical conductivity, and magnetic properties of rocks and minerals. Geophysical data can be utilized in mineral exploration for the subsequent objectives:

1. To ascertain the geographical areas where mineral resources are situated

2. To assess the magnitude and configuration of mineral reserves

3. Evaluate the caliber of mineral resources

Satellite data refers to visual representations of the Earth captured from outer space. This data enables the determination of the topography, vegetation, land use, and other attributes of the Earth's surface. Satellite data is utilized in mineral exploration for the following objectives:

1. Detect and recognize visible signs of mineral deposits on the Earth's surface.

2. To aid in the strategic organization of mineral exploration endeavors

3. To aid in the assessment of findings from mineral exploration

The integration of geological, geophysical, and satellite data is commonly employed in mineral exploration. By employing this approach, it becomes feasible to precisely and dependably identify and assess mineral resources.

Illustrative use cases

Geological data: Through field observations, surface manifestations of mineral deposits can be identified. Lead-zinc deposits typically manifest as minerals containing sulfur when observed on the surface. Geological observations in the field can be used to ascertain the existence of these minerals.

Geophysical data: Seismic methods are extensively employed in geophysics to ascertain the composition and characteristics of subsurface layers. Seismic methods can be employed to ascertain the existence and precise positioning of subterranean mineral deposits.

Satellite data: Satellite imagery is utilized to detect surface characteristics in the field of mineral exploration. Using infrared satellite images, it is possible to detect variations in vegetation. These variations could be linked to visible signs of mineral deposits on the surface.

Presently, the technologies employed in mineral exploration are steadily advancing. These advancements enable the implementation of mineral exploration activities with greater efficiency and effectiveness.

Machine Learning Theory in the Investigation of Mineral Deposits

Mineral exploration is a comprehensive process that is influenced by various geological, geochemical, and geophysical factors. The application of Machine Learning (ML) theory has become a potent tool for making decisions in the field of mineral exploration. Machine learning techniques, such as neural networks, random forests, and support vector machines, facilitate the detection of patterns and correlations in large datasets, allowing for systematic investigation. ML algorithms facilitate the integration and analysis of various datasets, allowing geologists and exploration teams to develop comprehensive models that improve comprehension of geological environments.

ML techniques are particularly effective in the classification of mineral deposits. Machine learning models can be trained to categorize various types of deposits by analyzing geological characteristics, geochemical compositions, and other distinctive factors. ML methodologies enhance production optimization through the prediction of production rates, identification of areas for operational improvement, and optimization of resource extraction processes. Nevertheless, achieving successful integration necessitates a sophisticated comprehension of geological principles and data science techniques. The successful application of geology relies heavily on the collaborative efforts between experts in the field and data scientists. The prudent incorporation of machine learning techniques has the potential to revolutionize the process of exploring, evaluating, and extracting mineral deposits, resulting in improved efficiency and sustainability in the mining sector.

Exploration process of Mineral Deposits with ML

The process of exploring and prospecting mineral deposits is highly intricate, and the application of machine learning theory can yield numerous advantages in this domain. Machine learning techniques can offer effective solutions in decision-making processes, exploration studies, classification of mineral deposits, and mineral production, as in various professional fields. The following text describes this process.

Data Analysis and Processing:

- Utilizing machine learning, large volumes of data obtained during the mineral exploration process can be analyzed and processed through the technique of big data analysis. This may encompass soil samples, geophysical data, geochemical data, and other geographical data.

- Pattern recognition: Machine learning can be employed to identify and categorize patterns that are indicative of the presence of minerals. This can facilitate the correlation of mineral deposits with distinct geographical characteristics.

Image processing and mapping:

- Satellite Imagery: Utilizing satellite imagery enables the identification of mineral deposits. Machine learning can assist in the identification of potential mineral deposits by analyzing distinctive characteristics present in these images.

- Mapping and Classification: Machine learning can be employed in the mineral exploration process to detect and categorize terrain characteristics in various regions. This can facilitate the identification of specific categories of mineral deposits.

Modeling and forecasting:

- Geophysical and geochemical data can be utilized for modeling purposes. Machine learning models can analyze these data

sets and accurately predict the location and dimensions of mineral deposits.

- Machine learning can be employed to evaluate risks in the mineral exploration process and identify the most effective exploration strategies.

Automated Decision Support Systems:

- Utilizing Artificial Intelligence for Decision Support: Machine learning can assist in making decisions during the mineral exploration process. This can facilitate the automation of decisions, such as the selection of sites, planning of drilling activities, and allocation of resources.

The utilization of machine learning in the exploration of mineral deposits offers numerous benefits. These benefits facilitate the process of mineral exploration and contribute to its long-term viability.

- Enhanced precision: Machine learning models exhibit superior accuracy in making predictions compared to conventional approaches. This enables miners to discover additional reserves while minimizing resource expenditure.

Utilizing machine learning for mineral exploration

- Enhanced search efficiency: Machine learning enables miners to precisely focus their search efforts on the desired area. This facilitates the discovery of additional reserves by mining companies, requiring less exertion and financial resources.

- Unearthing novel opportunities: Machine learning enables miners to identify previously unknown mineral deposits that are not detectable using conventional methods. This has the potential to generate fresh prospects for the mining sector.

Discussion

Machine Learning (ML) has transformed the investigation of mineral deposits by improving effectiveness, precision, and

comprehensiveness. Machine learning algorithms can handle large and diverse datasets from various sources. This allows for the development of comprehensive models that surpass traditional methods. Machine learning simplifies the process of identifying complex patterns and correlations in geological, geochemical, and geophysical data, allowing geologists to more precisely pinpoint potential mineralization zones. Machine learning-based predictive modeling is crucial for optimizing exploration strategies by prioritizing exploration targets, efficiently allocating resources, and reducing exploration costs. The integration of data from multiple sources and scales enhances our comprehensive comprehension of geological environments, thereby enabling well-informed decision-making in exploration efforts. Machine learning techniques also aid in the recognition and classification of different kinds of mineral deposits, facilitating the creation of models that can distinguish between unique geological characteristics and compositions. Predictive modeling enables the prediction of production rates, the optimization of extraction methods, and the identification of opportunities for operational improvement. This improves operational efficiency and supports the management of resources in a sustainable manner.

Machine learning (ML) is an expanding discipline in economic geology, with current research investigating its use in categorization (Gregory et al., 2019; Zhong et al., 2021a) and the identification of unusual geochemical patterns (Zuo, 2017). Nevertheless, economic geologists lacking a background in machine learning have faced limited availability of ML models to validate predictions against real-world geological data in practical scenarios. The study conducted by Sun et al. (2022) demonstrated the efficacy of machine learning techniques combined with mineral geochemistry in determining the genesis of the Qingchengzi Pb-Zn ore field in China. The deposits in this area are either metamorphosed sedimentary exhalative (SEDEX) or magmatic-hydrothermal fluid-related.

Geological mapping is a crucial process in mineral exploration. By utilizing both machine learning techniques and remote sensing data, it is possible to efficiently and affordably map lithological units, alteration zones, structures, and indicator minerals that are linked to mineral deposits (Sun and Scanlon, 2019). The rapid progress in obtaining high-resolution remote sensing data has resulted in a significant increase in big data (Sun and Scanlon, 2019), which presents new possibilities for discovery based on data analysis (Gewali et al., 2018).

Shirmard et al., 2022 present a thorough examination of how machine learning techniques are used in processing remote sensing data to model geological patterns and investigate ore deposits. The machine learning methods are categorized into five groups: dimensionality reduction, classification, clustering, regression, and deep learning methods. The paper also addresses obstacles and potential future research, with an interdisciplinary emphasis on recent advanced techniques in deep learning, including graph deep learning methods, Bayesian deep learning, variational autoencoders, and transformer recurrent neural networks.

Conclusion

Machine learning (ML) is essential in the field of mineral exploration as it enables data-driven decision-making, precise predictive modeling, and efficient classification of deposits. Nevertheless, the obstacles such as the accuracy of data and the comprehensibility of machine learning models necessitate a collaborative effort between geologists and data scientists from different fields. To overcome these challenges, it is crucial to enhance ML algorithms and promote collaboration among domain experts. The advancement of machine learning-driven methodologies offers great potential for the mining industry, expediting the identification of deposits and guaranteeing the implementation of environmentally responsible extraction techniques.

REFERENCES

Bishop, C. M. (2006). Pattern recognition and machine learning (Information science and statistics). Springer-Verlag New York, Inc.

Brynjolfsson, E., & McAfee, A. (2017). The business of artificial intelligence. Harvard Business Review, 1–20.

Chen, Q., & Zhao, P., (2011). Singularity theories and methods for characterizing mineralization processes and mapping geoanomalies for mineral deposit prediction. Geoscience Frontiers 2, 67–79.

Davies, R.S., David, I., Groves, D.I., Trencha, A., & Dentith, M. (2020). Towards producing mineral resource-potential maps within a mineral systems framework, with emphasis on Australian orogenic gold systems. Ore Geology Reviews 119, 103369.

Fischer, M., Heim, D., Hofmann, A., Janiesch, C., Klima, C., & Winkelmann, A. (2020). A taxonomy and archetypes of smart services for smart living. Electronic Markets, 30(1), 131–149. https:// doi.org/10.1007/s12525-019-00384-5.

Ford, A., & Hart, C.J. (2013). Mineral potential mapping in frontier regions: A Mongolian case study. Ore Geology Reviews 51, 15–26.

Ge, C., Huo, J., Gu, H.O., Wang, F., Sun, H., Li, X., Li, W., & Yuan, F. (2021). Tectonic discrimination and application based on convolution neural network and incomplete big data. J. Geochem. Explor. 220, 106662. https://doi.org/10.1016/j. gexplo.2020.106662.

Gewali, U.B., Monteiro, S.T., & Saber, E. (2018). Machine Learning Based Hyperspectral Image Analysis: A survey.

Ghezelbash, R., Maghsoudi, A., & Carranza, E.J.M. (2019). An Improved data-driven multiple criteria decision-making procedure for spatial modeling of mineral prospectivity: Adaption of

prediction–area plot and logistic functions. Natural Resources Research 28, 1299–1316.

Goodfellow, I., Bengio, Y., & Courville, A. (2016). Deep learning. The MIT Press.

Gregory, D.D., Cracknell, M.J., Large, R.R., McGoldrick, P., Kuhn, S., Maslennikov, V.V., Baker, M.J., Fox, N., Belousov, I., Figueroa, M.C., Steadman, J.A., Fabris, A.J., & Lyons, T.W., (2019). Distinguishing ore deposit type and barren sedimentary pyrite using laser ablation inductively coupled plasma-mass spectrometry trace element data and statistical analysis of large data sets. Econ. Geol. 114, 771– 786. https://doi.org/10.5382/econgeo.4654.

Gupta, R. (2020). A Survey on Machine Learning Approaches and Its Techniques, 2020 IEEE International Students' Conference on Electrical, Electronics and Computer Science (SCEECS), 2020, pp. 1-6, doi: 10.1109/ SCEECS48394.2020.190.

Hu, B., Zeng, L.P., Liao, W., Wen, G., Hu, H., Li, M.Y.H., & Zhao, X.F., (2022). The origin and discrimination of High-Ti magnetite in magmatic-hydrothermal systems: Insight from machine learning analysis. Econ. Geol. 117 (7), 1613–1627. https://doi.org/10.5382/econgeo.4946.

Huang, X.W., Boutroy, E., Makvandi, S., Beaudoin, G., Corriveau, L., & De Toni, A.F., (2019). Trace element composition of iron oxides from IOCG and IOA deposits: relationship to hydrothermal alteration and deposit subtypes. Miner. Deposita 54, 525–552. https://doi.org/10.1007/s00126-018-0825-1.

Jessell, M., Ailleres, L., Kemp, E., Lindsay, M., & Wellmann, F. (2014). Next generation three-dimensional geologic modeling and inversion. In: Kelley, K.D., Golden, H.C. (Eds.), Building Exploration Capability for the 21st Century. Society of Economic Geologists, pp. 261–272.

Jordan, M. I., & Mitchell, T. M. (2015). Machine learning: Trends, perspectives, and prospects. Science, 349(6245), 255–260. https://doi. org/10.1126/science.aaa8415.

Kreuzer, O.P., Etheridge, M.A., Guj, P., McMahon, M.E., & Holden, D. (2008). Linking mineral deposit models to quantitative risk analysis and decision-making in exploration. Economic Geology 103, 829–850.

Kreuzer, O.P., Yousefi, M., & Nykanen, V. (2020). Introduction to the special issue on spatial modelling and analysis of ore forming processes in mineral exploration targeting. Ore Geology Reviews 109, 10339. https://doi.org/10.1016/j. oregeorev.2020.103391.

Li, X.M., Zhang, Y.X., Li, K.Z., Zhao, X.F., Zuo, R.G., Xiao, F., & Zheng, Y. (2023). Discrimination of Pb-Zn deposit types using sphalerite geochemistry: New insights from machine learning algorithm, Geoscience Frontiers, Volume 14, Issue 4, 101580, ISSN 1674-9871, https://doi.org/10.1016/j.gsf.2023.101580.

Liu, L., Wan, C., Zhao, C., & Zhao, Y., (2011). Geodynamic constraints on orebody localization in the Anqing orefield, China: Computational modeling and facilitating predictive exploration of deep deposits. Ore Geology Reviews 43, 249–263.

Liu, L., & Qin, Y. (2019). 3D prediction by MLAs based on computational modeling in maturely explored area: A case study in Anqing orefield, China [ext. abs.]. in: Life with Ore Deposits on Earth: Proceedings of the 15th SGA Biennial Meeting, Glasgow, Scotland, 1278-1281.

Louppe, G., (2014). Understanding random forests: From Theory to Practice. Ph.D thesis, University of Liège, Belgium.

Mahesh, B. (2020). Machine Learning Algorithms-A Review. International Journal of Science and Research, 9, 381-386.

O'Sullivan, G., Chew, D., Kenny, G., Henrichs, I., & Mulligan, D. (2020). The trace element composition of apatite and

its application to detrital provenance studies. Earth Sci. Rev. 201, 103044. https://doi.org/10.1016/j.earscirev.2019.103044.

Parsa, M., & Carranza, E.J.M. (2021). Modulating the impacts of stochastic uncertainties linked to deposit locations in data-driven predictive mapping of mineral prospectivity. Natural Resources Research 30, 3081–3097.

Petrelli, M., & Perugini, D. (2016). Solving petrological problems through machine learning: the study case of tectonic discrimination using geochemical and isotopic data. Contrib. Miner. Petrol. 81, 171. https://doi.org/10.1007/s00410- 016-1292-2.

Qin, Y., & Liu, L. (2018). Quantitative 3D association of geological factors and geophysical fields with mineralization and its significance for ore prediction: An example from Anqing orefield, China. Mineral 8 (e 300), https://doi.org/10.3390/min8070300.

Russell, S. J., & Norvig, P. (2021). Artificial intelligence: A modern approach (4th ed.). Pearson.

Saha, R., Upadhyay, D., & Mishra, B. (2021). Discriminating tectonic setting of igneous rocks using biotite major element chemistry — A machine learning approach. Geochem. Geophys. Geosyst. 22, e2021GC010053. https://doi.org/10.1029/ 2021GC010053.

Shirmard, H., Ehsan Farahbakhsh, R. Müller, D., & Chandra, R. (2022). A review of machine learning in processing remote sensing data for mineral exploration, Remote Sensing of Environment, Volume 268, 112750, ISSN 0034-4257, https://doi.org/10.1016/j.rse.2021.112750.

Singer, D.A., & Kouda, R. (1999). Examining risk in mineral exploration. Nature Resources Research 8, 111–122.

Sun, G., Zeng, Q., & Zhou, X.J. (2022). Machine learning coupled with mineral geochemistry reveals the origin of ore deposits. Ore Geology Reviews. 142, 104753, ISSN 0169-1368, https://doi.org/10.1016/j.oregeorev.2022.104753.

Sun, A.Y., & Scanlon, B.R. (2019). How can big data and machine learning benefit environment and water management: a survey of methods, applications, and future directions. Environ. Res. Lett. 14, 73001. https://doi.org/10.1088/1748-9326/ ab1b7d

Ueki, K., Hino, H., & Kuwatani, T. (2018). Geochemical discrimination and characteristics of magmatic tectonic settings: A machine-learningbased approach. Geochem. Geophys. Geosyst. 19, 1327–1347. https://doi.org/ 10.1029/2017GC007401.

Ula, M. (2020). A Survey on The Accuracy of Machine Learning Techniques for Intrusion and Anomaly Detection on Public Data Sets. 2020 International Conference on Data Science, Artificial Intelligence, and Business Analytics (DATABIA) 2020 19 27 10.1109/DATABIA50434.2020.9190436

Wang, Y., Qiu, K.F., Mu¨ller, A., Hou, Z.L., Zhu, Z.H., & Yu, H.C., (2021b). Machine learning prediction of quartz forming-environments. J. Geophys. Res. Solid Earth 126. https://doi.org/10.1029/2021JB021925.

Wang, H., Ye, L., Hu, Y., Wei, C., Li, Z., Huang, Z., & Shuang, Y., (2021a). Trace element characteristics in sphalerites from the Laochangping Pb-Zn deposit in the Southeastern Chongqing. Acta. Mineral. Sin. 41, 623–634. https://doi.org/ 10.16461/j.cnki.1000-4734.2021.41.083. (in Chinese with English abstract)

Witherly, K. (2014). Geophysical expressions of ore systems — Our current understanding. in: Kelley, K. D., Golden, H. C., (Eds.), Building Exploration Capability for the 21st Century, Society of Economic Geologists, 176-208.

Yousefi, M., Carranza, E.J.M., Kreuzer, O.P., Nyk¨ anen, V., Hronsky, J.M.A., & Mihalasky, M.J. (2021). Data analysis methods for prospectivity modelling and applies to mineral exploration targeting: State-of-the-art and outlook. Journal of Geochemical Exploration 229, 106839. https://doi.org/10.1016/j. gexplo.2021.106839.

Zheng, D., Wu, S., Ma, C., Xiang, L., Hou, L., Chen, A., & Hou, M. (2022). Zircon classification from cathodoluminescence images using deep learning. Geosci. Front. 13 (6), 101436. https://doi.org/10.1016/j.gsf.2022.101436.

Zhong, R., Deng, Y., & Yu, C., (2021a). Multi-layer perceptron-based tectonic discrimination of basaltic rocks and an application on the Paleoproterozoic Xiong'er volcanic province in the North China Craton. Comput. Geosci. 149, 104717. https://doi.org/10.1016/j.cageo.2021.104717.

Zhong, R., Deng, Y., Li, W., Danyushevsky, L.V., Cracknell, M.J., Belousov, I., Chen, Y., & Li, L., (2021b). Revealing the multi-stage ore-forming history of a mineral deposit using pyrite geochemistry and machine learning-based data interpretation. Ore Geol. Rev. 133, 104079. https://doi.org/10.1016/j.oregeorev.2021.104079.

Zuo, R. (2017). Machine Learning of Mineralization-Related Geochemical Anomalies: A Review of Potential Methods. Nat. Resour. Res. 26 (4), 457–464.

CHAPTER V

Evaluation Of Gumushane Chrome Valley Şamanlı Chapel In Terms Of Ground Properties

Mahmut SARI[1]
Nurgül ŞENTÜRK [2]

Introduction

The ground properties of historical buildings and whether they were built according to the underground conditions of the area where they were built can be investigated using geophysical methods without damaging these structures. Prior to commencing the repair of ancient buildings, it is imperative to ascertain the ground properties (Sert et al., 2015). Significant structural damages

[1] Dr. Öğretim Üyesi, Gümüşhane Üniversitesi Meslek Yüksekokulu, İnşaat Bölümü, msari@gumushane.edu.tr ORCID:0000-0002-1006-6332
[2] Öğretim Görevlisi, Gümüşhane Üniversitesi Meslek Yüksekokulu, Tasarım Bölümü, nurgul.senturk@gumushane.edu.tr ORCID:0000-0003-4222-7265

observed in historical buildings, near-vertical cracks or splits due to ground settlements, and deformations related to earthquakes are the important ground problems encountered in these and similar structures (Erten and Mısırlı, 2023; Yüksel, 2009). Historical buildings are generally structures built using the masonry technique. Since there are no skeletal systems, all walls act as load-bearing curtains. While they exhibit remarkable resistance to compressive loads owing to their substantial structural weight, they typically struggle to withstand tensile stresses. As a result of these factors, deformations can arise from horizontal forces, such as earthquakes, in our country, which is situated on active fault lines (Akbaş and Çalışkan., 2023; Ma et al., 2022; Cengiz, 2022; Schmidt et al., 2015; Rosendahl et al., 2014; Sala et al., 2012; Gaffney and Gaffney, 2011; Gaffney, 2008; Linford and Canti, 2001).Climate-related rainfall regime causes floods in irregular regions and serious damage to stone arches. Settlement damage occurring on the floor can affect the entire system and cause cracks. In addition to all these effects, faulty repairs caused by humans, wars and fires cause deformation and deterioration of historical buildings (Murat and Yardımlı, 2021).

The Şamanlı chapel in the Şamanlı District within the Krom Valley of Yağlıdere Village was built on a low hill on a road surrounding the village. This study aimed to determine the ground properties of Şamanlı Chapel, including the locations and geological structure of the underground layers. Seismic methods, which are geophysical techniques, were employed to determine the seismic velocities, elastic properties, and dynamic parameters of the layers. As a result, the underground situation of the chapel was revealed. An assessment was conducted to determine if the evident structural faults in the Şamanlı chapel were caused by the ground.

Geology of Study Area

Gümüşhane is situated in the Eastern Black Sea Region and has borders with Bayburt to the east, Giresun to the west, Trabzon to the north, and Erzincan to the south. Gümüşhane has an average altitude of 1210 meters above sea level. The study location is situated

in the chrome valley inside the confines of Yağlıdere village, Merkez district, Gümüşhane province (Figure 1).

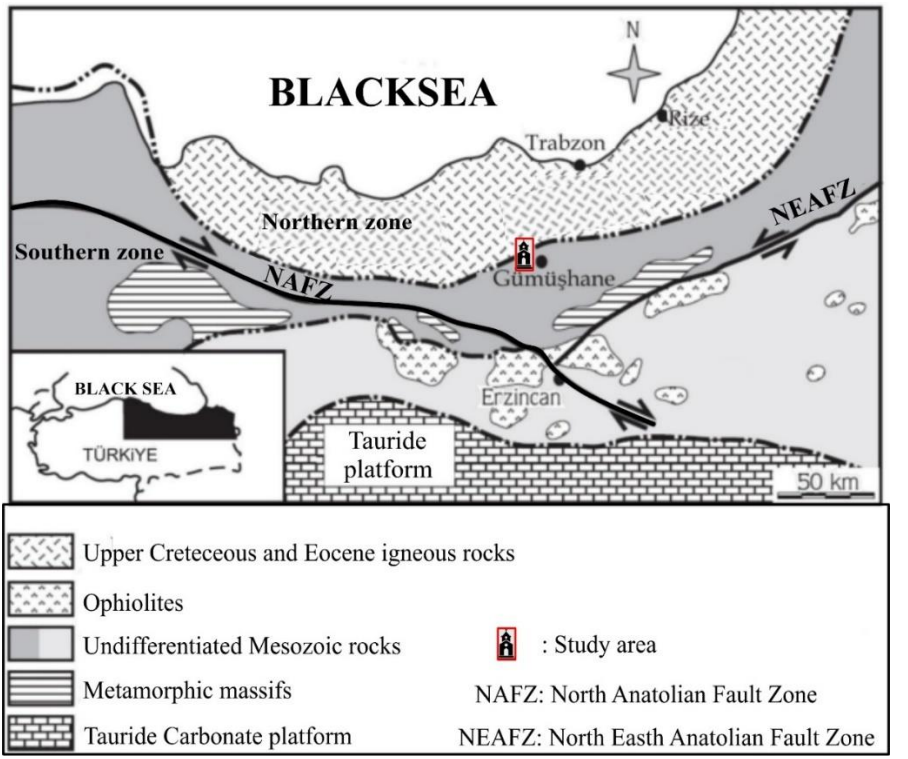

Figure 1. Geotectonic location of the study area (Bektas et al., 1987)

In the research region, there are exposed rock units that formed throughout the Paleozoic-Quaternary time period. Magmatism, which began in the Liassic period and continued until the end of the Eocene, is a typical occurrence (Ketin, 1950; Çoğulu, 1970). Additionally, volcanic and indurative rocks, as well as volcano-sedimentary rocks, are also present. Soot sedimentary deposits formed during periods of magmatic activity cessation (Yılmaz, 1972; Eren, 1983; Topuz vd., 2010).

In this part of the Eastern Pontides, sequences with different lithostratigraphic features are observed, namely the northern zone and the southern zone (Ketin, 1966). In the northern zone, from bottom to top, Paleozoic gneiss, micaschist, chloriteschist, etc. Metamorphites consisting of rocks, Liassic basalt, andesite, conglomerate, sandstone and marl etc. Hamurkesen formation consisting of rock types, Berdiga formation consisting of Upper Jurassic-Lower Cretaceous aged limestones, Upper Cretaceous aged basalt, andesite, pyroclastic, sandstone etc. Çatak formation consisting of rock types, Kızılkaya formation consisting of rhyodacite, dacite and pyroclastics, Kaçkar granitoid-I, basalt, andesite, pyroclastic, mudstone, sandstone, marl, etc. Çağlayan formation consisting of rock types, Çayırbağ formation consisting of rhyolite, rhyodacite and pyroclastics, Bakırköy formation consisting of Paleocene aged sandstone, marl and clayey limestone, Eocene aged Kaçkar granitoid-II and Kabaköy formation consisting of andesite, basalt and pyroclastics. The southern zone exhibits the Hamurkesen (Ağar, 1977) and Berdiga formations, while the northern zone is characterized by the Kaçkar granitoid-I-II and Kabaköy formation. In contrast, the Mescitli formation is present in a distinct manner (Figure 2).

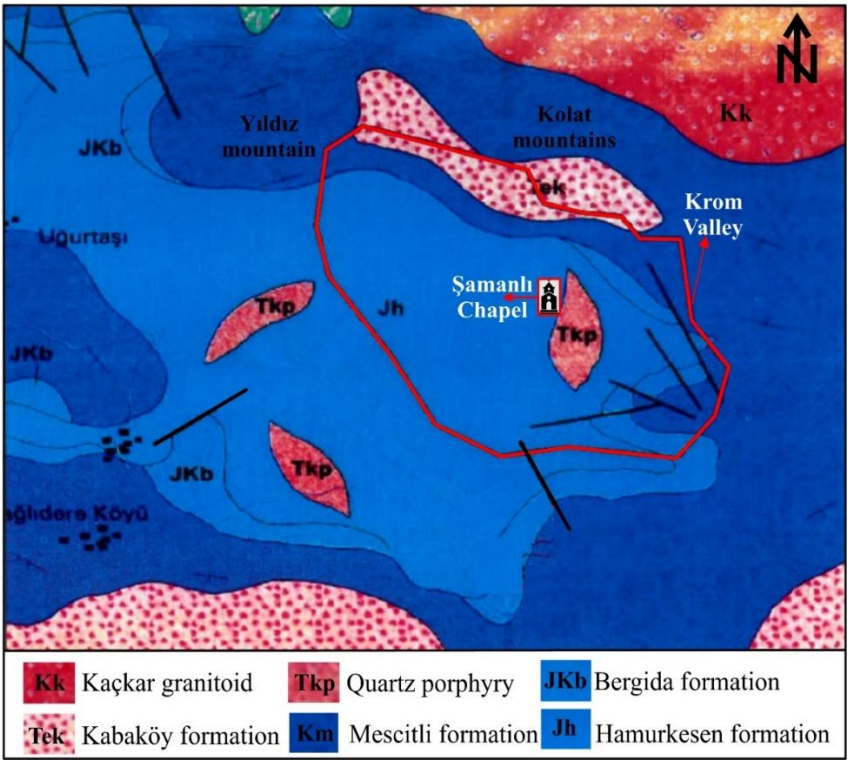

Figure 2. Geological map of the study area (modified from MTA geological map)

Methodology and Instrumentation

Seismic Refraction and Multi-Channel Surface Wave (MASW) measurements were conducted on a road profile adjacent to the Şamanlı Chapel in the research region (Figure 3).

Figure 3. The present-day photographs of Şamanlı Chapel

In the measurements taken, V_p and V_s velocity information was obtained from a distance of 78 m and a depth of approximately 30 m. The data gathering process involved the utilization of a Geometrics brand seismograph instrument with 24 channels, vertical component receivers with a frequency of 4.5 Hz, an 8 kg sledgehammer, and an iron table with a radius of 25 cm. At each shot location, four vertical stacks were constructed to enhance the signal-to-noise ratio of the seismic signal (Figure 4).

Figure 4. Seismic refraction and MASW methods line direction measurement layout

The seismic refraction and MASW data were sampled at intervals of 0.250 ms and 0.5 ms, respectively. The recording time for the data was 0.5s for seismic refraction and 1s for MASW. The offset interval for the data was 3m for seismic refraction and 9m for MASW. In order to evaluate the seismic refraction data upon first arrival, shots were made from the beginning, end and middle of the profile. No filter was used during data collection.

Using the V_p and V_s velocities of the layers in each profile, dynamic elasticity modulus (E_{dyn}) and dynamic poisson ratio (ν_{dyn}) values were calculated with the help of equations 1, 2 and 3 suggested by Bowles (1988) (Table 1). The shear modulus value was determined with the help of empirical equation number 3 suggested by Keçeli (2012). The density value was determined with the help of empirical equation number 4 suggested by Keçeli (2012).

$$\upsilon_{dyn} = (V_p{}^2 - 2V_s{}^2) / 2(V_p{}^2 - V_s{}^2) \quad \text{(Eq.1)}$$

$$E_{dyn} = \mu\,(3V_p{}^2 - 4V_s{}^2) / (V_p{}^2 - V_s{}^2) \quad \text{(Eq.2)}$$

$$\mu = \rho\, V_s{}^2 / 100 \quad \text{(Eq.3)}$$

$$\rho = 0.44 V_s{}^{0,25} \quad \text{(Eq.4)}$$

Here, V_p: P wave velocity (m/s), V_s: S wave velocity (m/s), ρ: density (gr/cm^3), υ: Poisson ratio, μ: shear modulus (kg/cm^2) and E_m is the modulus of elasticity (kg/cm^2).

Result and Discussions

Seismic refraction and MASW data were evaluated with the SeisImager program. After the first arrival times were correctly peaked in the seismic refraction analyses, the two-dimensional seismic velocity depth section of the shallow underground structure was obtained by subjecting it to inversion processing in the computer environment (Figure 5).

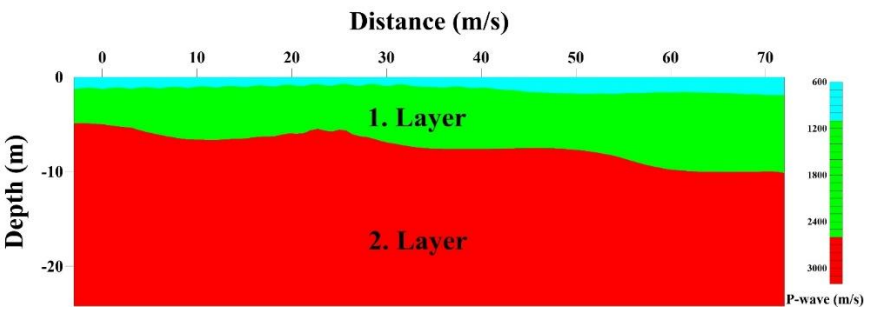

Figure 5. Two-dimensional Seismic refraction velocity and depth section

In MASW analyses, phase velocity and dispersion curves were determined by subjecting them to frequency-wavenumber analysis, and 1-dimensional S-wave velocity values varying with underground depth were obtained (Figure 6). The research area involved seismic measurements to determine the V_p and V_s wave velocities of the units within the shallow subsurface structure. The average V_p wave velocity value for the 1st Layer shown in green is 1470 m/s, V_s wave velocity value is 801 m/s. For the 2nd layer shown in red, the average V_p wave velocity value was determined as 2510 m/s and the Vs wave velocity value was 1377 m/s. Engineering parameters calculated based on velocity values obtained from geophysical methods are given in Table 1.

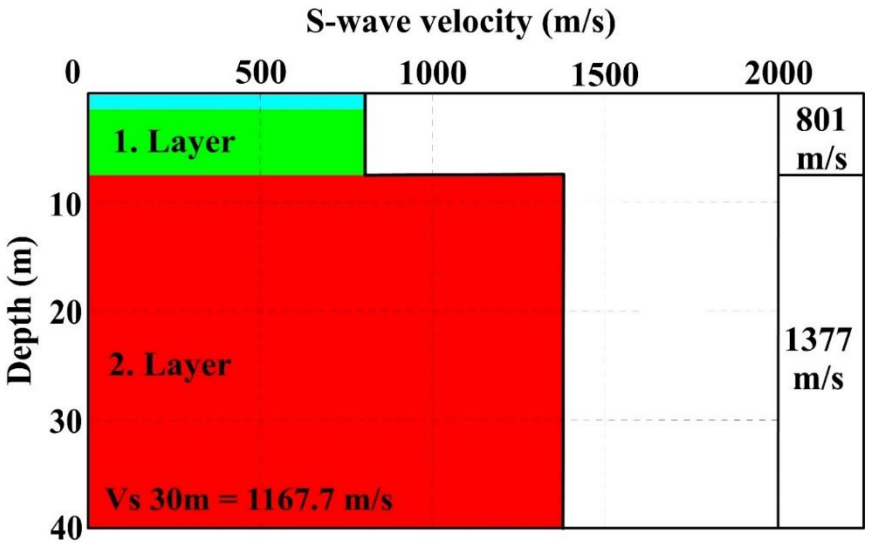

Figure 6. 1-dimensional MASW velocity and depth section

Table 1. Engineering parameters obtained in geophysical methods

DYNAMIC AND ELASTIC PARAMETERS									
Layer No.		**Vp (m/sec)**		**Vs (m/sec)**		**Vp / Vs**		**Layer Thickness (m)**	
1		1470		801		1,84		7,50	
2		2510		1377		1,82		30,50	
Density		**Poisson's Ratio**		**Shear Modulu**		**Elasticity Modulu**		**Bulk Module**	
gr/cm³	**Characterize**		**Firmness**	**kg/cm²**	**Strength**	**kg/cm²**	**Strength**	**kg/cm²**	**Compression**
1,92	high	(,29	strict	12319	very solid	31755	very solid	25064	middle
1,19	high	(,28	strict	41525	very solid	106696	very solid	82605	high

Geophone interval	**Offset interval**	**Dominant frequency (Ao)**		**Vs30**	**a**	**b**	**Dominant period**
(m)	**(m)**	**Midorikawa**	**Borcherdt et al. 1991**	**(m/sec)**			**(To - sec)**
3,00	6,00	1,00	0,60	1167	(,07	0 ,15	0,10

Taking into account the shear wave speed determined by taking MASW measurements on 1 line covering the examination area next to the Şamanlı chapel (TBDY, 2018), the units of the Hamurkesen formation according to the ground class in the Turkish Building Earthquake Regulation (TBDY) table; In the light of the information obtained as a result of MASW measurements, it was determined that the soil type with an average speed of Vs30m of 1167.7 m/s was in the ZB "Less weathered, medium solid rocks" group.

The closest active fault to the study area is KAFZ and the distance to the active fault varies between 70-80 km. Due to its proximity to the NAFZ, the study area is a region that has the potential to be affected by major earthquakes that may occur in this zone.

It is seen that the dominant period obtained from seismic velocity values in the study area is 0.1 s, and the TA and TB values of this period are 0.07 and 0.15 s, respectively. These values show the Z1 soil class according to the TBDY.

When the engineering parameters obtained from all geophysical methods were evaluated, it was concluded that there was no damage caused by any bad ground conditions, as the ground of the Şamanlı Chapel was built on a very solid, tight and high-strength rock ground. The visible structural damages are believed to be the result of anthropogenic factors, such as water infiltration, the decay of stones due to their overall deterioration, and the presence of clay layers or other foreign substances. These factors lead to ruptures and separation in the affected areas.

Conclusions

Gümüşhane Chrome Valley Şamanlı Chapel was evaluated in terms of soil properties and the results are given below.

- Seismic velocity values of Şamanlı Chapel obtained using seismic methods were determined as V_p: 1470 m/s, V_s: 801 m/s

for the first layer, V_p: 2510 m/s, V_s: 1377 m/s for the second layer.

- The soil was defined by determining the obtained velocity values and the Poisson ratio, shear modulus, elasticity modulus, Bulk modulus, dominant frequency (A_0) and dominant period (T_0) parameters.
- It is seen that the dominant period obtained from the seismic velocity values is 0.1 s, and the TA and TB values of this period are 0.07 and 0.15 s, respectively. These values have been determined to indicate Z1 soil class according to the TBDY.
- Units of the Hamurkesen formation according to ground class; In the light of the information obtained as a result of MASW measurements, it was determined according to TBDY that the soil type with an average speed of Vs30m was 1167.7 m/s and was in the ZB "Less weathered, medium solid rocks" group.
- Based on the engineering characteristics acquired, it was determined that the Şamanlı Chapel was constructed on a stable and robust bedrock, indicating that no damage was caused by unfavorable ground conditions. The visible structural damages are believed to be a result of human activities, water infiltration into the structure, the decay of the stones due to their overall deterioration, and the presence of clay layers or other foreign substances in the stones, leading to ruptures and separations in these areas. The Şamanlı Chapel has likely experienced varied degrees of structural degradation over time, including changes in function and deterioration caused by physical forces, throughout its existence.

References

Ağar, Ü. (1977). Demirözü (Bayburt) ve Köse (Kelkit) Bölgesi'nin Jeolojisi. *Doktora Tezi, KTÜ, Fen Bilimleri Enstitüsü*, Trabzon.

Akbaş, A., & Çalışkan, Ö. (2023). Deprem Etkisinde Hasar Alan Betonarme Yapıların Düzensizlik Türleri Yönü İle İncelenmesi. *In International Conference on Scientific and Academic Research* (Vol. 1, pp. 428-435).

Bektaş, O., Van, A. Boynukalın, S. (1987). Doğu Pontidlerde Jura Volkanizması ve Pontidler Jeotektoniğinde Yeri, *TJK Bülteni* 30-2, 9-19.

Cengiz, H. A. (2022). XVIII. Yüzyılda Edirne'de Yaşanan Taşkınların Köprülerde Oluşturduğu Hasarlar Üzerine Bir Araştırma. *Anadolu ve Balkan Araştırmaları Dergisi*, 5(9), 127-148.

Çoğulu, E. (1970). Gümüşhane ve Rize Granitik Plütonlarının Mukayeseli Petrolojik ve Jeokronolojik Etüdü, *Doçentlik Tezi, İTÜ Maden Fakültesi*, İstanbul.

Eren, M., (1983). Gümüşhane-Kale Arasının Jeolojisi ve Mikro fasiyes incelemesi Yüksek Lisans Tezi, KTÜ, Fen Bilimleri Enstitüsü, Trabzon.

Erten, Ş. Y., & Mısırlı, A. (2023). Yığma Yapılarda Gözleme Dayalı Bozulma/Hasar Tespiti: Eski Harbiye Kışlası. *Bayburt Üniversitesi Fen Bilimleri Dergisi*, 6(1), 38-50.

Gaffney C, Gaffney V. (2011). Through an imperfect fi lter: geophysical techniques and the management of archaeological heritage. *In: Cowley DC (ed) EAC Remote Sensing for Archaeological Heritage Management*, Occasional P.

Gaffney C. (2008). Detecting trends in the prediction of the buried past: A review of geophysical techniques in archaeology. *Archaeometry* 50: 313-336

Ketin, İ. (1966). Anadolu'nun Tektonik Birlikleri *MTA Dergisi Sayı*:66 MTA Ankara

Ketin, İ. (1950). Bayburt Bölgesinin Jeolojisi, İÜ, Fen Fakültesi Mecmuası, 16 İstanbul.

Linford NT, Canti MG. (2001). Geophysical evidence for fi res in antiquity: preliminary results from an experimental study. Paper given at the XXIV General Assembly in The Hague, April 1999. *Archaeological Prospection* 8: 211-225

Ma, S., Wang, L., Bao, P. (2022). Study on Properties of Blue-Brick Masonry Materials for Historical Buildings. Journal of Renewable Materials, 10(7), 1961–1978.

Murat, D. A. L., & Yardımlı, S. (2021). Taş Duvarlarda Yüzey Bozunmaları. *Kent Akademisi*, 14(2), 428-451.

Sala R, Garcia E, Tamba R. (2012). Archaeological geophysics – from basics to new perspectives. *In: OllichCastanyer I (ed) Archaeology, New Approaches in Theory and Techniques*. InTech. pp 133-166

Sert, H., Partal, E. M., Nas, M., Yılmaz, S., Demirci, H., Avşin, A., & Turan, G. S. (2015). Tarihi köprülerin restorasyonları kapsamında yürütülen yapısal analiz çalışmaları ve sonuçları. 5. Tarihi Eserlerin Güçlendirilmesi ve Geleceğe Güvenle Devredilmesi Sempozyumu, 1-3.

Schmidt A, Linford P, Linford N, David A, Gaffney C. (2015). EAC Guidelines for the use of Geophysics in Archaeology: Questions to Ask and Points to Consider. *Archaeolingua*, 138 pp

Rosendahl, D., K. Lowe, L. Wallis and S. Ulm. (2014). Integrating geoarchaeology and magnetic susceptibility at three shell mounds: a pilot study from Mornington Island, Gulf of Carpentaria, Australia. Journal of Archaeological Science 49:21–32

TBDY, 2018. https://www.resmigazete.gov.tr/eskiler/2018/03/20180318M1-2.htm

Topuz G., Altherr, R., Siebel W. ve Schwarz, W.H. (2010). Carboniferous High-Potassium I-Type Granitoid Magmatism in the Eastern Pontides, The Gümüşhane Pluton, NE Turkey, *Lithos,* 116, 92-110.

Yılmaz, Y. (1972). Gümüşhane Plütonunun ayrıntılı incelenmesi, M.T.A raporu, Yayın No: 2326, Ankara, 24.

Yüksel, F. A. (2009). Tarihi Yapıların Restorasyonlarında Jeofizik Yöntemlerin Kullanılması Metodolojisi. Restorasyon ve Konservasyon Çalışmaları Dergisi, 1(2), 62-67.

CHAPTER VI

Prediction of Capillary Water Absorption (CWA) Values for Pyroclastic Rocks Using Gene Expression Programming (GEP)

Mehmet Can BALCI[1]
İsmail İNCE[2]

Introduction

Natural stones are materials commonly used for structures constructed for defence, beliefs and residential purposes from the past to the present day. From the moment natural stones are quarried, they are exposed to atmospheric processes and deterioration processes begin. The presence of water within the building stone

[1] Assistant Professor, Batman University, Faculty of Engineering and Architecture, Department of Civil Engineering, Batman, Turkey
[2] Associate Professor, Konya Technical University, Faculty of Engineering and Natural Sciences, Department of Geological Engineering, Konya, Turkey

triggers and accelerates deterioration processes (İnce, 2021). Water within the building stone enters through transportation with the effect of capillary water absorption forces acting on water from rain and/or groundwater. A variety of features (low kinematics, index-mechanical properties, structural and textural properties etc) of the rock control the capillary water absorption of building stones (Tomašićet et al., 2011; Ozcelik and Ozguven, 2014; Sengun et al., 2014; Çobanoğlu, 2015; Bao and Wang, 2017; Pötzl et al., 2018; Unal and Altunok, 2019). Determining the capillary water absorption (CWA) value of building stones may be listed among important information for determining locations where the stone can be used and about deterioration processes. Several researchers examined simple regression correlations between CWA with index-strength and textural features of building stones (Vazquez et al., 2010; Stück et al., 2011; Dinçer et al., 2012; Sengun et al., 2014; İnce, 2021). Some researchers predicted the CWA values of building stones using artificial neural network (ANN), fuzzy and support vector regression (Çobanoğlu, 2015; İnce et al., 2021; Zhao et al., 2023; Miao et al., 2023; Yu and Wei, 2023; Ding, 2023; Qian et al., 2023). Gene expression programming (GEP) was proposed by Ferreira (2001) and is a prediction method commonly used in several disciplines (geology, environmental and civil engineering, biology) in recent times (İnce et al., 2019). In this study, the CWA values were predicted with GEP using index values for pyroclastic rocks.

Material and Method

For this study, 21 pyroclastic rock samples were collected from quarries in different regions of Anatolia. To prepare cube samples for use in the experimental stage, building stone blocks with dimensions of 30 × 30 × 30 cm were obtained from the quarries. For detection of the features of the building stones, cube samples with edge length 70 mm were prepared from these blocks.

The prepared samples had P-wave velocity, dry density, porosity and CWA tests performed. For determination of the P-wave velocity of the building stones, the standards recommended in

ASTM E494 (2010) were noted. The dry density and porosity values of the samples were identified by paying attention to methods recommended in TS EN-1936 (2010). The CWA values of the building stones were examined on the basis of the TS EN-1925 (2000) standard. From the moment the base of the cube samples contacted water, the water absorption amounts per unit area (g/m^2) were measured at the time intervals recommended in the standard (1, 3, 5, 10, 15, 30, 60, 480 and 1440 minutes). Measurements ended when the variation between two sequential measurements was less than 1%. Later, graphs of the square root of time ($t^{1/2}$) against water absorption amount per unit area (g/m^2) were drawn and the CWA value was determined for each sample from the slopes of the graphs.

Genetic Expression Programming (GEP) Approach

The GEP approach was developed by Ferreira in 2001. GEP was developed using the main principles of two programs (genetic algorithm and genetic programming). According to Ferreira (2001), in the GEP application, individuals code linear sequences of a genome with fixed dimensions. Later, non-linear clusters with different shapes and dimensions are defined and these are called expression trees (ETs). The gene chromosomes in GEP generally comprise two sections forming the head and tail. These entities are known as ET's, which are the expression of a chromosome. GEP chromosomes generally comprise more than one gene with equal length and each gene is divided into two sections of head and tail. The ETs for the GEP model developed to predict the CWA values of pyroclastic rocks are shown in Figure 1.

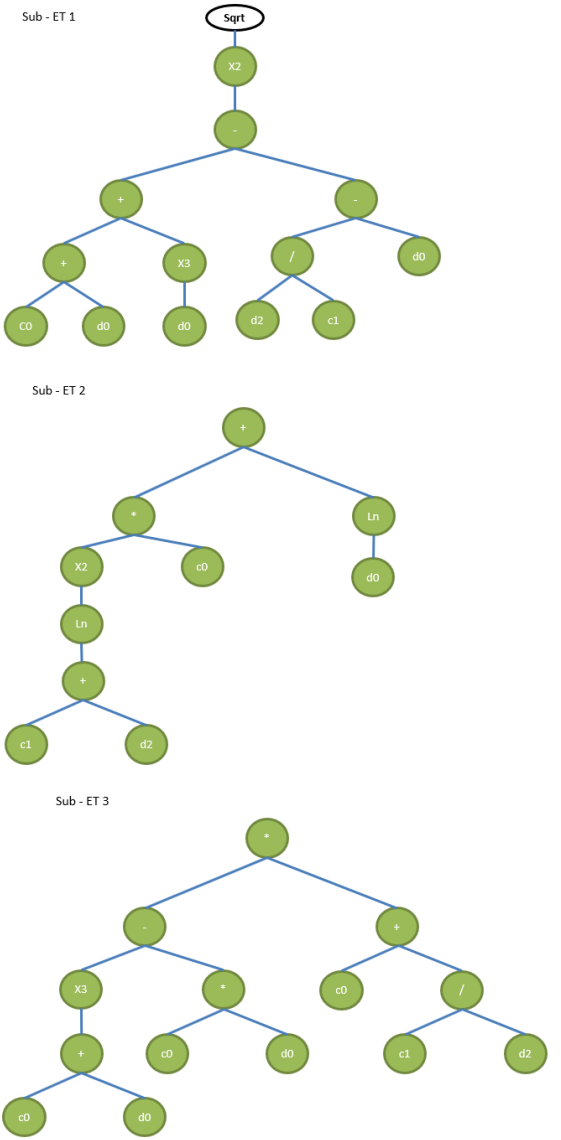

Figure 1. Expression Tree of GEP Model

In this GEP model, the number of genes and head length were 3 and 8, respectively (Table 1). During this process, multiplication

is used as connective process. During training and confirmation of the GEP model, Vp, ρ_d and n values were defined as input variables, while the CWA value was defined as the output variable (Table 1). In this study, 50 pyroclastic rock samples were used. To predict the CWA values of pyroclastic rocks with the GEP method, the Gene X pro Tools 4.0 software was used. The parameters chosen for the GEP model to predict the CWA value of building stones are given in Table 1. The constants for the developed model are presented in Table 2.

Table 1. Parameters of GEP Approach Models

Parameter definition	GEP
Function set	+, -, *, /, Sqrt, ln, x^2, x^3
Chromosomes	30
Head size	8
Number of genes	3
Linking function	Multiplication
Mutation rate	0.044
Inversion rate	0.1
One-point recombination rate	0.3
Two-point recombination rate	0.3
Gene recombination rate	0.1
Gene transposition rate	0.1

Table 2. The Input, Output Quantities and Constants Used in GEP Model

Input variables		Constants	
d0	ρ_d - g/cm^3	G1c0	-8.398773
d1	n - %	G1c1	0.580963
d2	Vp- km/s	G2c0	-0.256531
		G2c1	-0.226379
Output variable		G3c0	-4.597229
CWA	g/m^{2}s$^{0.5}$	G3c1	-8.837983

Results and Discussion

Some Indexes Properties of Building Stones

The statistical data related to P-wave velocity, porosity, dry density and CWA values among the index features of pyroclastic rocks used in the study are given in Table 3. The porosity values for the pyroclastic rocks used in the study varied over a broad interval of 12.13-38.30, while dry density values varied from 1.16 g/cm^3 to 2.19 g/cm^3. According to the NBG (1985) classification, these samples are defined as very low-density rocks with high and very high porosity.

The highest P-wave velocity value for the pyroclastic rocks was 4.00 km/s, with lowest P-wave velocity of 0.70 km/s. According to the CWA classification of Snethlage (2005), samples were included in the low and high absorption rock classes. The CWA values of the samples used in the study vary in a very wide range from 5.32 to 533.29 g/m^{2}s$^{0.5}$.

Table 3. Properties of Pyroclastic Rocks Used in The Study

Rock Properties	Minimum	Maximum	Mean	Std. Deviation
Vp - km/s	0.70	4.00	2.44	0.80
n - %	12.13	38.30	22.41	7.60
ρ_d – g/cm^3	1.16	2.19	1.76	0.26
CWA- (g/m^{2}s$^{0.5}$	5.32	533.29	145.74	124.43

Prediction of Capillary Water Absorption Values of Pyroclastic Rocks

In this study, a prediction model using the GEP program for CWA values of 21 pyroclastic rocks collected from Anatolia was developed. In the model, 75% of the sample cluster (16 samples) was allocated for training, while 25% of the dataset (5 samples) was used to test the developed model. Three parameters of mean squared error (MSE), root mean squared error (RMSE) and correlation coefficient (R^2) were used to check the reliability of the developed equation (Equations 1-3).

$$MSE = \sum_{t=1}^{n}(o_i)^2, \quad (1)$$

$$RMSE = \sqrt{\frac{1}{n}\sum_{i=1}^{n}(t_i - o_i)^2}, \quad (2)$$

$$R^2 = \frac{(n\sum t_i o_i - \sum t_i \sum o_i)^2}{(n\sum t_i^2 - (\sum t_i)^2)(n\sum o_i^2 - (\sum o_i)^2)}. \quad (3)$$

Where *n* is total data number, *o* is calculated value and *t* is experimental value.

The statistical parameters for the training and test sets for the GEP model developed to predict the CWA values of pyroclastic rocks are given in Table 4. For the training set of the GEP model, the MSE, RMSE and R^2 values were 679.23, 26.06 and 0.96, respectively (Figure 2a). For the test set of the GEP model, the MSE values was 1108.29, the RMSE value was 33.29 and the R^2 value was 0.91 (Figure 2b).

Table 4. The CWA Statistical Values of GEP Model

Statistical parameters	GEP	
	Training set	Testing set
MSE	679.2382	1108.2935
RMSE	26.0622	33.2910
R^2	0.9624	0.9164

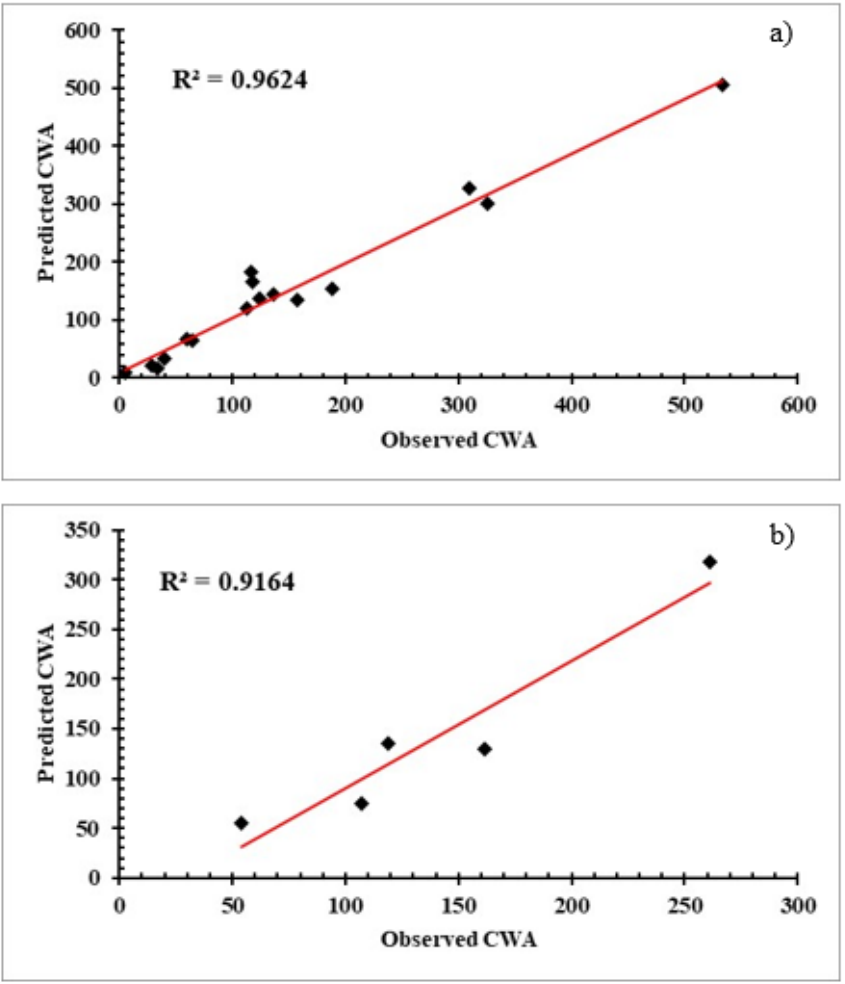

Figure 2. Comparison of CWA Experimental Results with Results of GEP Model; a) Training, b) Testing

Conclusion

Pyroclastic rocks are components forming the cultural texture with common use as building materials for many years due to outcropping over large areas of the Earth, ease of processing and

low density. The CWA values of these building stones, which vary over a large interval, cause different responses to deterioration processes. The importance of determining the CWA value, the most effective parameter in the deterioration process, has increased. This study developed a GEP model with the aim of predicting the CWA values for 21 different pyroclastic rocks using index features (Vp, ρ_d, and n).

- The GEP model developed for the assessed samples successfully predicted the CWA value. Statistical values like MSE, RMSE and R^2 proved this consistency.

- The R^2 values for the training and test sets for the developed GEP model were higher than 0.91.

- Due to the proposed GEP model, the CWA value, determined with difficult and time-consuming methods, can be predicted without any experiments.

With more detailed and comprehensive studies, the types of equations developed in this study for pyroclastic rocks collected from the Anatolian region will be evaluated by increasing the number and diversity of samples. It is recommended to evaluate the usability of similar index properties in determining CWA values of pyroclastic rocks from other parts of the world.

REFERENCES

ASTM E494. (2010). Standard Practice for Measuring Ultrasonic Velocity in Materials. ASTM International, West Conshohocken

Bao, J., & Wang, L. (2017). Capillary imbibition of water in discrete planar cracks. *Construction and Building Materials*, 146, 381-392.

Çobanoğlu, İ. (2015). Prediction and identification of capillary water absorption capacity of travertine dimension stone. *Arabian Journal of Geosciences*, 8, 10135-10149.

Dinçer, İ., Özvan, A., Mutluhan, A. K. I. N., Tapan, M., & Vural, O. Y. A. N. (2012). İgnimbiritlerin kapiler su emme potansiyellerinin değerlendirilmesi: Ahlat Taşı örneği. *Yüzüncü Yıl Üniversitesi Fen Bilimleri Enstitüsü Dergisi*, 17(2), 64-71.

Ding, M. (2023). Hybrid regression models: predicting of the capillary water absorption properties of construction stones. *Multiscale and Multidisciplinary Modeling, Experiments and Design*, 1-15.

EN, T. (2010). Natural stone test methods-Determination of real density and apparent density and of total and open porosity. *Turkish Standards Institute, Ankara, Turkey*, 10.

En, T. S. (2000). Natural stone test methods-Determination of water absorption coefficient by capillarity. *CNR-ICR, Rome*.

Ferreira, C. (2001). Gene expression programming: a new adaptive algorithm for solving problems. *arXiv preprint cs/0102027*.

İnce, İ., Bozdağ, A., Fener, M., & Kahraman, S. (2019). Estimation of uniaxial compressive strength of pyroclastic rocks (Cappadocia, Turkey) by gene expression programming. *Arabian Journal of Geosciences*, 12, 1-13.

İnce, İ. (2021). Relationship between capillary water absorption value, capillary water absorption speed, and capillary rise

height in pyroclastic rocks. *Mining, Metallurgy & Exploration*, 38(2), 841-853.

İnce, İ., Bozdağ, A., Barstuğan, M., & Fener, M. (2021). Evaluation of the relationship between the physical properties and capillary water absorption values of building stones by regression analysis and artificial neural networks. Journal of Building Engineering, 42, 103055.

Miao, Y., Liu, Z., Zhuang, Z., & Yan, X. (2023). Hybrid ANFIS models were used to calculate the capillary water absorption values of construction stones. *Journal of Intelligent & Fuzzy Systems*, (Preprint), 1-11.

Ozcelik, Y., & Ozguven, A. (2014). Water absorption and drying features of different natural building stones. *Construction and building materials*, 63, 257-270.

Pötzl, C., Siegesmund, S., Dohrmann, R., Koning, J. M., & Wedekind, W. (2018). Deterioration of volcanic tuff rocks from Armenia: constraints on salt crystallization and hydric expansion. *Environmental earth sciences*, 77, 1-36.

Qian, D., Yang, J., & Wang, J. (2022). Novel hybrid models to predict the capillary water absorption values of building stones. *Engineering Research Express*, 4(3), 035012.

Sengun, N., Demirdag, S., Akbay, D., Ugur, I., Altindag, R., & Akbulut, A. (2014, October). Investigation of the relationships between capillary water absorption coefficients and other rock properties of some natural stones, V. In Global stone congress (pp. 22-25).

Snethlage, R. (2005). Leitfaden Steinkonservierung, Fraunhofer IRB, Stuttgart, p. 289.

Stück, H., Siegesmund, S., & Rüdrich, J. (2011). Weathering behaviour and construction suitability of dimension stones from the Drei Gleichen area (Thuringia, Germany). *Environmental Earth Sciences*, 63, 1763-1786.

Tomašić, I., Lukić, D., Peček, N., & Kršinić, A. (2011). Dynamics of capillary water absorption in natural stone. Bulletin of Engineering Geology and the Environment, 70, 673-680.

Unal, M., & Altunok, E. (2019). Determination of water absorption properties of natural building stones and their relation to porosity. *Engineering Sciences*, 14(1), 39-45.

Vázquez, P., Alonso, F. J., Esbert, R. M., & Ordaz, J. (2010). Ornamental granites: Relationships between p-waves velocity, water capillary absorption and the crack network. Construction and Building Materials, 24(12), 2536-2541.

Yu, B., & Wei, Y. (2023). A comparison study of regression analysis for estimating the capillary water absorption of construction stones. *Multiscale and Multidisciplinary Modeling, Experiments and Design*, 1-12.

Zhao, G., Wang, H., & Li, Z. (2023). Capillary water absorption values estimation of building stones by ensembled and hybrid SVR models. *Journal of Intelligent & Fuzzy Systems*, 44(1), 1043-1055.

CHAPTER VII

Journey from the Depths of the Earth to the Surface: Kimberlites

Mustafa Eren RİZELİ

Introduction

Kimberlites are fascinating geological formations with mysterious allure beneath the Earth's surface. Named after the town of Kimberley in South Africa, where they were first discovered, these igneous rocks have captivated scientists and gem enthusiasts alike for their role in the formation of diamonds. Kimberlites are not just rocks; they are conduits of Earth's deep-seated processes, bringing precious minerals from the mantle to the surface. Understanding the unique characteristics and origins of kimberlites sheds light on the intricate dynamics that govern the Earth's geology and the remarkable journey of diamonds from the planet's depths to the hands of humans.

This compilation study was conducted to explain what kimberlites are, the geological processes involved in their formation, and the issues related to kimberlite-diamond relations in light of current studies.

Methodology

A rigorous research methodology was employed to compile comprehensive information on kimberlites and their association with diamonds, drawing from various scientific books, peer-reviewed articles, theses, and reputable online resources. The following steps were undertaken to ensure the accuracy and reliability of the gathered information: Scientific books devoted to geology, mineralogy and petrology were extensively reviewed, focusing on chapters discussing kimberlites and diamond formation (1). Peer-reviewed journal articles investigating the geological processes involved in forming kimberlites and the development of diamonds within these structures were analysed. It was aimed to obtain findings about kimberlite and diamonds by examining master's and doctoral theses (2). Searches were conducted in reputable online sources, including academic databases and scientific websites, to gather up-to-date information and recent advances in understanding kimberlites and diamond relationships (3).

This compilation study uses the above methodology to synthesise kimberlites and their complex connection to diamond formation. We aim to draw on the academic community's latest scientific research and understanding.

Geological processes in the formation of kimberlites

Kimberlites, uncommon igneous rocks (Fig. 1), are found in the form of volcanic diatremes, dykes, and sills within enduring and stable continental areas (Mitchell, 1986; Giuliani and Pearson, 2019). Kimberlites originate in specific regions of the Earth's mantle called diamond stability zones. These zones are characterised by high temperatures and pressures conducive to the diamonds'

stability. The process begins with the partial melting of the mantle rocks within these diamond stability zones. The exact mechanisms triggering this partial melting are not fully understood, but it is believed to be related to changes in pressure, temperature, and the presence of volatile substances such as water (Tappe et al., 2018; Pearson et al., 2019; Castillo-Oliver et al., 2020). The partially melted material gives rise to a unique type of magma known as kimberlitic magma. Kimberlitic magmas are distinct for their high volatile content, including water, carbon dioxide, and other gases. The composition of these magmas plays an important role in their explosive nature and ability to transport diamonds to the surface (Mitchell, 2008).

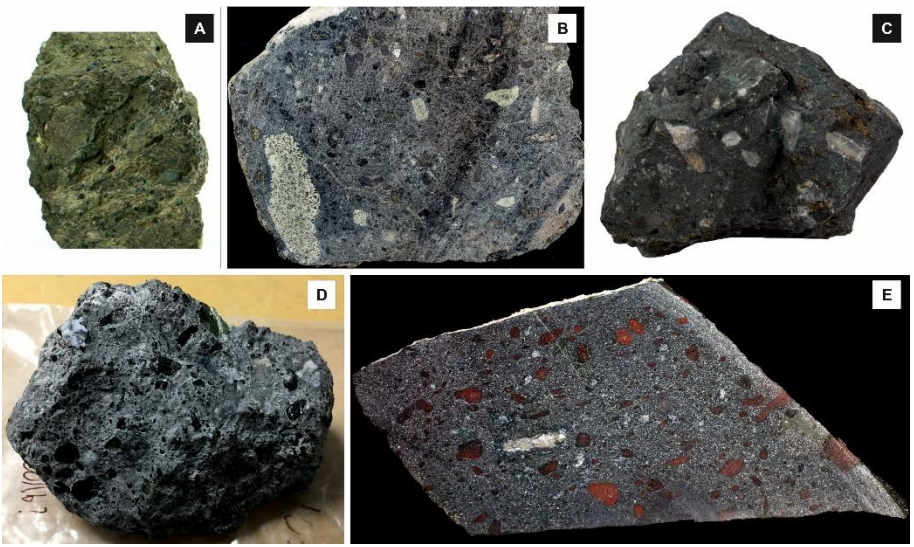

Figure 1. Hand specimens of kimberlites. (A) Kimberley, South Africa; (B) Monastery Mine, South Africa; (C-D) Udachnaya open-pit mine, Russia; (E) Kelsey Lake, State Line Kimberlite Mining District, Colorado, USA (Mindat, 2023)

Kimberlitic magma rises rapidly through narrow, pipe-like conduits in the Earth's crust. It carries mantle material, including xenoliths (fragments of surrounding rocks) and diamonds. The rapid ascent and eruption bring these materials from the mantle to the

Earth's surface (Mitchell, 1986; Wilson and Head, 2007; Russell et al., 2012, 2019). Ascent speed is critical in preserving diamonds, as rapid ascent prevents them from transforming into graphite during the journey. The ascent is thought to be facilitated by the buoyancy of the volatile-rich magma. The kimberlitic magma reaches the Earth's surface, resulting in a violent and explosive eruption. This process creates volcanic landforms known as kimberlite pipes or diatremes (Seib et al., 2013). These pipes are characterised by a brecciated (fragmented) rock matrix containing various minerals, including diamonds (Mitchell et al., 2019). The chart in Figure 1 shows the structure of an ideal kimberlite suggested by Mitchell (1986).

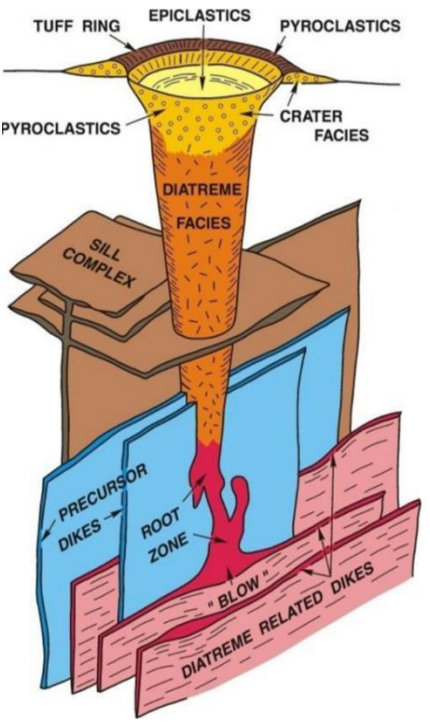

Figure 2. Illustration of an idealised kimberlite system, demonstrating the hypabyssal, diatreme, and crater facies (Mitchell, 1986).

It is important to note that the formation of kimberlites is a dynamic and intricate geological process, and researchers continue to investigate the details of each stage. The study of kimberlites provides valuable insights into the deep Earth processes and the journey of diamonds from the mantle to the Earth's surface (Mitchell, 1986; Griffin et al., 1999, 2004; Russell et al., 2012; Aulbach et al., 2018; Moss et al., 2018; Giuliani and Pearson, 2019).

Types of kimberlites

There is ongoing controversy regarding the specific composition of kimberlite melts (Foley et al., 2019; Pearson et al., 2019; Mitchell et al., 2019), and similar debates surround the crystallisation conditions of kimberlite. Smith (1983) categorised kimberlites into two groups, Group I and Group II, based on variations in their isotopic composition.

Group I comprises the most classical kimberlites initially referred to as basaltic kimberlites. These are ultrabasic rocks with low silica content (SiO_2 < 45 wt%), high levels of potassium (K/Na atomic ratio > 1), and rich in volatiles, predominantly carbon dioxide (CO_2). They are characterised by the presence of large and very large crystals (macro- and megacrysts) of magnesium-rich minerals such as olivine, pyropic garnet, ilmenite, alternately chromium-rich diopsidic pyroxene, enstatite, titanium-poor chromite, and phlogopite. These crystals are embedded in a fine matrix consisting of olivine, carbonate, serpentine, and magnesium- and/or calcium-rich minerals. It is noteworthy that both the macro- and megacrysts are, at least in part, xenocrysts, meaning they are accidental crystalline components originating from the disruption of country-rocks, essentially deep-seated mantle peridotites, and eclogites, intersected by the ascending kimberlite magma (Smith, 1983).

Group II kimberlites, or orangeites, were originally labelled micaceous or lamprophyric kimberlites. These rocks are ultrapotassic (with a K/Na ratio exceeding 3), peralkaline (with [K + Na]/Al greater than 1), and rich in volatiles, primarily water (H_2O).

They are characterised by the presence of macro-crysts composed of phlogopite and olivine, set in a groundmass containing diopside, phlogopite, and olivine, often exhibiting zoning to titanian aegirine. Additionally, the groundmass contains spinel with compositions ranging from magnesium-bearing chromite to titanium-bearing magnetite, perovskite, and other minerals. Notably, Group II kimberlites exhibit a mineralogical similarity to lamproites rather than Group I kimberlites (Smith, 1983).

The global occurrence of kimberlites

Kimberlites are distributed across all continents worldwide (see Fig. 4). Analysing the global distribution of kimberlites, economically significant kimberlites are primarily located on Pre-Cambrian Cratons, specifically those with an Archaean age (older than approximately 2.5 billion years; Clifford, 1966). Clifford's Rule, as it came to be known, highlights no documented instances of primary diamond deposits in crustal terrains that are less than 1.6 billion years old. The distinctive correlation implies a link between the existence of diamonds and the age of the subcontinental lithosphere. Clifford's rule is widely recognised as an important guideline in initiatives related to diamond exploration. It is important to highlight that diamonds found in kimberlite are generally of a more recent age when compared to the lithospheric region they penetrate. Examples range from Cretaceous occurrences, including many in South Africa, to Palaeozoic instances (such as those in Siberia), and the entire spectrum stretches from the Proterozoic to the Neogene, encompassing instances like the 22-million-year-old examples in Western Australia.

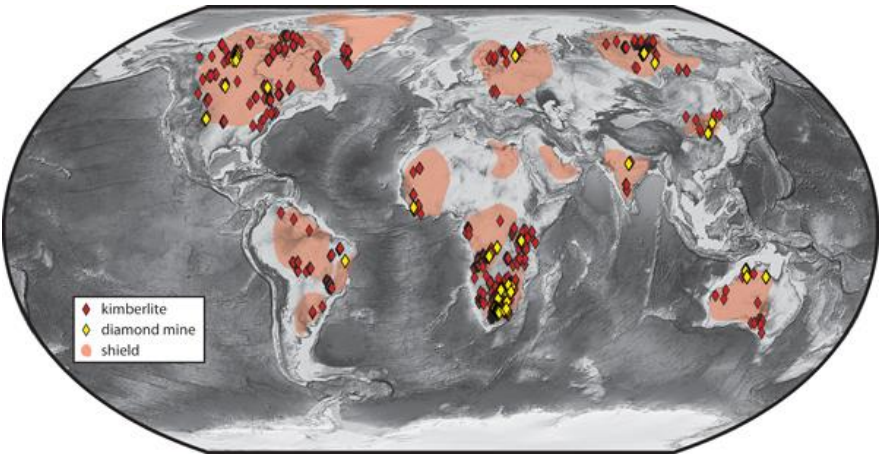

Figure 3. A worldwide elevation map displays the presence of kimberlites (Giuliani and Pearson, 2019 and references therein)

It is important to note that while kimberlites are widespread, not all contain economically viable quantities of diamonds. High-quality diamonds and favourable mining conditions often determine the economic significance of kimberlite deposits. Additionally, the distribution of kimberlites is subject to ongoing exploration and discovery efforts, with new occurrences occasionally identified.

The Economic significance and global impact of kimberlites

Kimberlites serve as the primary geological formations containing diamonds (Fig. 4), constituting over 70% of the total diamond value and representing the primary source for most commercial diamond production. These diamonds do not come from the magma itself (phenocrysts); rather, they are external crystals (xenocrysts) transported by a kimberlitic magma as it rises towards the Earth's surface (Harte and Cayzer, 2007; Mitchell et al., 2019).

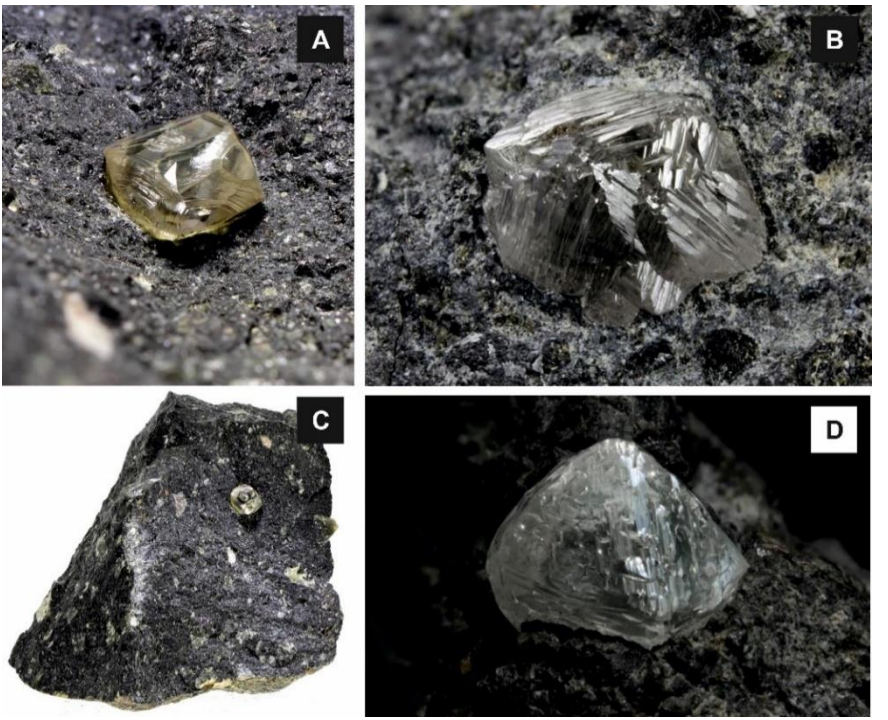

Figure 4. Diamonds in kimberlites from Bultfontein Mine, Kimberley, South Africa (Alexstrekeisen, 2023)

The exploration and mining of kimberlites are closely intertwined with the history of diamond research. Before 1865, diamonds were only obtained from alluvial deposits in Brazil and India. The finding of alluvial diamonds in South Africa in 1866 sparked a diamond rush, eventually uncovering primary diamond deposits in 1869 on farms that would later become the townships of Jagersfontein, Koffiefontein, and Kimberley (Field et al., 2008). The systematic mining operations at the Bultfontein, Dutoitspan, De Beers, and Kimberley deposits marked the initial indication that the rocks hosting diamonds had an igneous origin. These structures were later designated as "kimberlites," a name derived from the town of Kimberley, where these deposits were situated (Lewis, 1887). However, it was not until the 1950s and 1960s, with the discovery of

kimberlites beyond southern Africa in places like the USA and Russia, that the worldwide importance of kimberlite magmatism was entirely recognised. The modern discovery of kimberlites was significantly supported by Peter H. Nixon's influential book "Lesotho Kimberlites" (Nixon, 1973).

Currently, around 3,500 kimberlites have been recognised and distributed across every continent worldwide (Fig. 3). Moreover, diamond exploration companies estimate the existence of approximately 3,000 additional kimberlites. Most of these occurrences are located in the stable cores of continents, particularly in the Archean cratons and the adjacent mobile belts. The connection between diamond-bearing kimberlites and cratons (or peri-cratonic areas) was identified by Kennedy in the 1960s and later termed "Clifford's rule." Kimberlites are frequently associated with significant lithospheric structures, such as sutures between continental blocks and shear zones. They are commonly located at the intersections of intersecting lineaments (e.g., Jelsma et al., 2009). The rise of kimberlite magma takes advantage of pre-existing areas of mechanical vulnerability in the upper lithosphere.

Out of the kimberlites identified so far, only 3% exhibit significant diamond content, which contains macro-diamonds with a grade exceeding 1 carat per hundred tons (de Wit, 2010). A modest number, less than 100 kimberlites, has been subjected to large-scale commercial diamond mining. This includes a few olivine lamproites, encompassing rocks formerly categorised as "Group II kimberlites " or orangeites," hosting diamond mines like Finsch in South Africa and Argyle in Western Australia. Several factors influence the economic viability of a kimberlite, including (1) the diamond grade, which refers to the concentration of diamonds within the kimberlite rock mass; (2) the quality of diamonds, primarily assessed by their average size, clarity, and colour; (3) the size of the ore body; and (4) the local environment, encompassing climate, infrastructure, and political stability (Kjarsgaard, 2007). Evaluating the economic viability and the practicality of extracting resources from a

kimberlite formation presents a significant challenge (Kjarsgaard et al., 2007).

In summary, kimberlites have significant economic and commercial implications, primarily driven by the extraction and trade of diamonds. The diamond industry, in turn, influences various sectors, including job creation, infrastructure development, and investment opportunities. However, balancing economic gains with environmental and social considerations is important to ensure long-term sustainability.

Results

Kimberlites, named after the South African town of Kimberley, are intriguing geological formations playing a crucial role in the formation of diamonds. This study aims to elucidate kimberlites, their geological processes, and their association with diamonds by compiling current research. Kimberlites, uncommon igneous rocks, form in volcanic diatremes, dykes, and sills within stable continental areas. Originating in diamond stability zones in the Earth's mantle, partial melting, influenced by pressure, temperature, and volatile substances, gives rise to kimberlitic magma. This magma, rich in volatiles, ascends rapidly through conduits, carrying mantle material, xenoliths, and diamonds. The explosive eruption creates kimberlite pipes on the Earth's surface, preserving diamonds due to rapid ascent. Controversy surrounds kimberlite melt compositions. Smith categorised them into Group I (basaltic kimberlites) and Group II (orangeites). Group I exhibits ultrabasic, volatile-rich characteristics, while Group II is ultrapotassic, peralkaline, and water-rich, resembling lamproites. Kimberlites are globally distributed, with economically significant deposits primarily on Pre-Cambrian Cratons, supporting Clifford's Rule. While widespread, not all kimberlites contain economically viable diamonds, and exploration efforts continue. Kimberlites constitute over 70% of the total diamond value and are the primary source for commercial diamond production. They play a pivotal role in the history of diamond research. A small percentage of identified

kimberlites have significant diamond content. Economic viability depends on factors such as diamond grade, quality, ore body size, and local conditions. In summary, kimberlites represent a dynamic geological process crucial to the diamond industry. Their economic significance underscores their impact on various sectors, necessitating a balance between economic gains and environmental and social considerations for long-term sustainability.

REFERENCES

Alexstrekeisen, (2023). *Kimberlites 2023.* (Accessed on 06/18/2023 from https://www.alexstrekeisen.it/english/vulc/kimberlites.php)

Aulbach, S., Creaser, R.A., Stachel, T., Heaman, L.M., Chinn, I.L., Kong, J. (2018). Diamond ages from Victor (Superior Craton): Intra-mantle cycling of volatiles (C, N, S) during supercontinent reorganisation. *Earth Planet. Sci. Lett.*, 490, 77–87. Doi: 10.1016/j.epsl.2018.03.016

Castillo-Oliver, M., Giuliani, A., Griffin, W.L., O'Reilly, S.Y., Drysdale, R.N., Abersteiner, A., Thomassot, E., Li, X.-H. (2020). New constraints on the source, composition, and post-emplacement modification of kimberlites from in situ C–O–Sr-isotope analyses of carbonates from the Benfontein sills (South Africa). *Contrib. to Mineral. Petrol.*, 175, 33. Doi: 10.1007/s00410-020-1662-7

Clifford, T.N. (1966). Tectono-metallogenic units and metallogenic provinces of Africa. *Earth Planet. Sci. Lett.*, 1, 421–434. https://doi.org/10.1016/0012-821X(66)90039-2

de Wit, M. (2010). Identification of global diamond metallogenic clusters to assist exploration. In: The 4th Colloquium on Diamonds—Source to Use 2010. Southern African Institute of Mining and Metallurgy, Johannesburg, Republic of South Africa, pp 15-38

Field, M., Stiefenhofer, J., Robey, J., Kurszlaukis, S. (2008). Kimberlite-hosted diamond deposits of southern Africa: A review. *Ore Geol. Rev.*, 34, 33–75. Doi: 10.1016/j.oregeorev.2007.11.002

Foley, S.F., Yaxley, G.M., Kjarsgaard, B.A. (2019). Kimberlites from Source to Surface: Insights from Experiments. Elements 15, 393–398. Doi: 10.2138/gselements.15.6.393

Giuliani, A., & Pearson, D. G. (2019). Kimberlites: From Deep Earth to Diamond Mines. *Elements*, 15 (6), 377–380. Doi: 10.2138/gselements.15.6.377

Griffin, W.L., Batumike, J.M., Greau, Y., Pearson, N.J., Shee, S.R., O'Reilly, S.Y. (2014). Emplacement ages and sources of kimberlites and related rocks in southern Africa: U–Pb ages and Sr–Nd isotopes of groundmass perovskite. *Contrib. to Mineral. Petrol.* 168, 1032. Doi: 10.1007/s00410-014-1032-4

Griffin, W.L., Shee, S.R., Ryan, C.G., Win, T.T., Wyatt, B.A. (1999). Harzburgite to lherzolite and back again: metasomatic processes in ultramafic xenoliths from the Wesselton kimberlite, Kimberley, South Africa. *Contrib. to Mineral. Petrol.* 134, 232–250. Doi: 10.1007/s004100050481

Harte, B., Cayzer, N. (2007). Decompression and unmixing of crystals included in diamonds from the mantle transition zone. *Phys. Chem. Miner.,* 34, 647–656. Doi: 10.1007/s00269-007-0178-2

Jelsma, H., Barnett, W., Richards, S., Lister, G. (2009). Tectonic setting of kimberlites. *Lithos* 112, 155–165. Doi: 10.1016/j.lithos.2009.06.030

Kennedy, W.Q. (1964). *The Structural Differentiation of Africa in the Pan-African (±500 m.y.) Tectonic Episode.* Leeds University Research Institute of African Geology and Department of Earth Sciences Annual Report on Scientific Results, 8, 48-49.

Kjarsgaard, B.A. (2007). Kimberlite diamond deposits, in Good fellow, W.D., ed., Mineral Deposits of Canada: A Synthesis of Major Deposit Types, District Metallogeny, the Evolution of Geological Provinces, and Exploration Methods: Geological Association of Canada, Mineral Deposits Division, Special Publication No. 5, p. 245-272.

Lewis, H.C. (1887). On a diamondiferous peridotite and the genesis of diamond. *Geological Magazine,* 5, 22–24

Mindat, (2023). *Kimberlite 2023*. (Accessed on 05/18/2023 from https://www.mindat.org/gm/48035)

Mitchell, R. H. (1986). *Kimberlites*. *Mineralogy, Geochemistry, and Petrology*. London: Plenum Press.

Mitchell, R.H. (2008). Petrology of hypabyssal kimberlites: Relevance to primary magma compositions. *J. Volcanol. Geotherm. Res.* 174, 1–8. Doi: 10.1016/j.jvolgeores.2007.12.024

Mitchell, R.H., Giuliani, A., O'Brien, H. (2019). What is a Kimberlite? Petrology and Mineralogy of Hypabyssal Kimberlites. *Elements,* 15, 381–386. Doi: 10.2138/gselements.15.6.381

Moss, S.W., Kobussen, A., Powell, W., Pollock, K. (2018). Kimberlite emplacement and mantle sampling through time at A154N kimberlite volcano, Diavik Diamond Mine: lessons from the deep. Mineral. Petrol., 112, 397–410. Doi: 10.1007/s00710-018-0630-7

Nixon, P. H., (1973). *Lesotho kimberlites*. Lesotho: Lesotho National Development Corporation

Pearson, D.G., Woodhead, J., Janney, P.E. (2019). Kimberlites as Geochemical Probes of Earth's Mantle. *Elements,* 15, 387–392. Doi: 10.2138/gselements.15.6.387

Russell, J.K., Porritt, L.A., Lavallée, Y., Dingwell, D.B. (2012). Kimberlite ascent by assimilation-fuelled buoyancy. *Nature,* 481, 352–356. Doi: 10.1038/nature10740

Russell, J.K., Sparks, R.S.J., Kavanagh, J.L. (2019). Kimberlite Volcanology: Transport, Ascent, and Eruption. *Elements,* 15, 405–410. Doi: 10.2138/gselements.15.6.405

Seib, N., Kley, J., Büchel, G. (2013). Identification of maars and similar volcanic landforms in the West Eifel Volcanic Field through image processing of DTM data: efficiency of different methods depending on preservation state. *Int. J. Earth Sci.*, 102, 875–901. Doi: 10.1007/s00531-012-0829-5

Smith, C.B. (1983). Pb, Sr and Nd isotopic evidence for sources of southern African Cretaceous kimberlites. *Nature* 304, 51–54. Doi: 10.1038/304051a0

Tappe, S., Smart, K., Torsvik, T., Massuyeau, M., de Wit, M., (2018). Geodynamics of kimberlites on a cooling Earth: Clues to plate tectonic evolution and deep volatile cycles. *Earth Planet. Sci. Lett*. 484, 1–14. Doi: 10.1016/j.epsl.2017.12.013

Wilson, L., Head III, J.W. (2007). An integrated model of kimberlite ascent and eruption. *Nature* 447, 53–57. Doi: 10.1038/nature05692